Acute or Delayed Systemic Administration of Human Amnion Epithelial Cells Improves Outcomes in Experimental Stroke

Megan A. Evans, PhD; Rebecca Lim, PhD; Hyun Ah Kim, PhD; Hannah X. Chu, PhD; Chantelle V. Gardiner-Mann, BSc(Hons); Kimberly W.E. Taylor, BSc(Hons); Christopher T. Chan, PhD; Vanessa H. Brait, PhD; Seyoung Lee, PhD; Quynh Nhu Dinh, PhD; Antony Vinh, PhD; Thanh G. Phan, MD, PhD; Velandai K. Srikanth, MD, PhD; Henry Ma, MD; Thiruma V. Arumugam, PhD; David Y. Fann, PhD; Luting Poh, BSc(Hons); Cameron P.J. Hunt, PhD; Colin W. Pouton, PhD; John M. Haynes, PhD; Stavros Selemidis, PhD; William Kwan, BBiomedSc(Hons); Leon Teo, PhD; James A. Bourne, PhD; Silke Neumann, PhD; Sarah Young, PhD; Emma K. Gowing, BSc(Hons); Grant R. Drummond, PhD; Andrew N. Clarkson, PhD; Euan M. Wallace, MD; Christopher G. Sobey, PhD*; Brad R.S. Broughton, PhD*

Background and Purpose—Human amnion epithelial cells (hAECs) are nonimmunogenic, nontumorigenic, anti-inflammatory cells normally discarded with placental tissue. We reasoned that their profile of biological features, wide availability, and the lack of ethical barriers to their use could make these cells useful as a therapy in ischemic stroke.

Methods—We tested the efficacy of acute (1.5 hours) or delayed (1–3 days) poststroke intravenous injection of hAECs in 4 established animal models of cerebral ischemia. Animals included young (7–14 weeks) and aged mice (20–22 months) of both sexes, as well as adult marmosets of either sex.

Results—We found that hAECs administered 1.5 hours after stroke in mice migrated to the ischemic brain via a CXC chemokine receptor type 4-dependent mechanism and reduced brain inflammation, infarct development, and functional deficits. Furthermore, if hAECs administration was delayed until 1 or 3 days poststroke, long-term functional recovery was still augmented in young and aged mice of both sexes. We also showed proof-of-principle evidence in marmosets that acute intravenous injection of hAECs prevented infarct development from day 1 to day 10 after stroke.

Conclusions—Systemic poststroke administration of hAECs elicits marked neuroprotection and facilitates mechanisms of repair and recovery.

Visual Overview—An online visual overview is available for this article. **(*Stroke*. 2018;49:700-709. DOI: 10.1161/STROKEAHA.117.019136.)**

Key Words: brain ischemia ■ cerebral infarction ■ inflammation ■ mice ■ stem cells

The majority of patients with ischemic stroke are ineligible to receive the only approved drug treatment, recombinant tissue-type plasminogen activator, because it must be administered within 4.5 hours of stroke onset,[1] and so new therapies that can be commenced beyond this window are desperately needed. Although a plethora of compounds that target single receptors or pathways have shown promise in preclinical models, none have been effective in clinical stroke trials.[2] Given the complex nature of postischemic brain injury and its systemic consequences,[2,3] cell-based approaches could achieve greater efficacy than single pharmacological therapies through targeting of multiple mechanisms.[4] Indeed, although a range of cell types can rescue injured

Received August 22, 2017; final revision received December 14, 2017; accepted December 15, 2017.

From the Departments of Pharmacology (M.A.E., H.A.K., H.X.C., C.V.G.-M., K.W.E.T., C.T.C., V.H.B., S.L., Q.N.D., A.V., G.R.D., C.G.S., B.R.S.B.), Obstetrics and Gynaecology (R.L., E.M.W.), Surgery (A.V., G.R.D., C.G.S.), and Medicine (T.G.P., V.K.S.), Australian Regenerative Medicine Institute (W.K., L.T., J.A.B.), and Monash Institute of Pharmaceutical Sciences (C.P.J.H., C.W.P., J.M.H.), Monash University, Victoria, Australia; Department of Physiology, Anatomy and Microbiology, La Trobe University, Victoria, Australia (M.A.E., H.A.K., Q.N.D., A.V., G.R.D., C.G.S.); The Ritchie Centre, Hudson Institute of Medical Research, Victoria, Australia (R.L., E.M.W.); Stroke Unit (T.G.P., V.K.S., H.M.) and Monash Women's Services (E.M.W.), Monash Health, Victoria, Australia; Menzies Research Institute, Tasmania, Australia (V.K.S.); Department of Physiology, Yong Loo Lin School of Medicine, National University of Singapore (T.V.A., D.Y.F., L.P.); School of Pharmacy, Sungkyunkwan University, Seoul, South Korea (T.V.A.); School of Health and Biomedical Sciences, RMIT University, Victoria, Australia (S.S.); Department of Anatomy, Brain Health Research Centre and Brain Research New Zealand (S.N., E.K.G., A.N.C.) and Department of Pathology (S.N.;S.Y.;A.N.C.), University of Otago, Dunedin, New Zealand; and Faculty of Pharmacy, University of Sydney, NSW, Australia (A.N.C.).

*Drs Sobey and Broughton contributed equally.

The online-only Data Supplement is available with this article at http://stroke.ahajournals.org/lookup/suppl/doi:10.1161/STROKEAHA.117.019136/-/DC1.

Correspondence to Christopher G. Sobey, PhD, Department of Physiology, Anatomy, and Microbiology, School of Life Sciences, La Trobe University, Victoria 3086, Australia. E-mail c.sobey@latrobe.edu.au

brain and improve recovery in models of stroke,[4] limited cell supplies, invasive extraction procedures, immunologic rejection, tumorigenesis, and ethical and logistical problems will likely prevent the use of most as viable routine treatment options.[5]

Human amnion epithelial cells (hAECs) have received almost no attention as a potential stroke therapy but offer many advantages. These placenta-derived cells possess pluripotent differentiation ability, immunomodulatory properties, are in ready supply (placentae are usually discarded after birth), are harvested noninvasively, and have virtually no ethical barriers to their use.[6] Likely reflecting their role in maintaining maternal immune tolerance of the fetus during pregnancy, hAECs are immunologically inert and have a low risk of rejection on transplantation. Also, hAECs do not express telomerase and therefore do not generate tumors on transplantation.[5,7] Furthermore, compared with other amnion-derived stem cell types (ie, amnion mesenchymal cells), hAECs can be isolated in vast abundance (hundreds of millions compared with tens of thousands), circumventing the need for ex vivo expansion of cells. Moreover, from a clinical translation perspective, hAECs represent a significantly lower cost than amnion mesenchymal cells because therapeutic doses can be obtained within hours of placenta collection, as opposed to weeks of culture expansion. Indeed, hAECs can promote neuroprotection during the acute phase of neuronal injury and facilitate neuroregeneration in models of central nervous system disorders.[8,9] We are currently evaluating hAECs in a phase I Clinical Trial for bronchopulmonary dysplasia (Australian New Zealand Clinical Trials Registry: ACTRN12614000174684).

Here, we show that intravenous delivery of hAECs can reduce ischemic brain damage and promote functional recovery when administered as late as 3 days after ischemic stroke in immunocompetent mice. We demonstrate that hAECs mediate their protective and proreparative effects via modulating immune cells that coordinate the inflammatory response to cerebral ischemia. These actions seem to be independent of both age and sex because hAECs are beneficial in young male and aged female mice. Finally, we show proof-of-principle evidence that poststroke treatment with hAECs can limit infarct development in a nonhuman primate model of ischemic stroke.

Methods

Data supporting the findings of this study are available from the corresponding author on reasonable request.

Study Design

Here, we have tested the efficacy of systemically delivered hAECs in established animal models of ischemic stroke. These studies were performed in support of several STAIRs[10] and STEPs[11] recommendations (Stroke Treatment Academic Industry Roundtable [STAIR]; Stem Cell Therapy as an Emerging Paradigm in Stroke [STEPS]) and used models of transient and permanent cerebral ischemia, young and aged animals of both sexes, and nonhuman primates. We assessed different time points at which hAECs could be delivered after stroke. See Figure I in the online-only Data Supplement for experimental timelines outlining the models of stroke used in this study.

Animals

Studies were approved by Monash University and University of Otago Animal Ethics Committees. A total of 326 male C57Bl6 mice (7–14 weeks old), 68 female C57Bl6 mice (20–22 months old), and 6 timed pregnant female C57Bl6 mice were used. We also studied 6 New World marmoset monkeys (*Callithrix jacchus*; 3–5 years; 2 females, 4 males).

Experimental Models

Most mice were subjected to either sham surgery or filament-induced right middle cerebral artery occlusion (MCAO) for 30 minutes, and the filament was then retracted to allow reperfusion (transient MCAO). Some cohorts were subjected to 60 minutes of MCAO to confirm efficacy of hAECs after a stronger ischemic insult and reperfusion. Groups were only compared with others subjected to the same period of MCAO. Alternatively, the filament was not retracted to induce permanent MCAO. Other mice were subjected to sham surgery or focal stroke of the left primary motor cortex induced by photothrombosis. In marmosets, stroke was produced in the left primary visual cortex by targeted intracortical injections of endothelin-1 proximal to the calcarine artery to cause transient arterial occlusion. Detailed descriptions, and a discussion of the comparative features of the mouse and marmoset models of cortical stroke, are in the online-only Data Supplement.

Administration of hAECs

hAECs were isolated from term placentae donated by healthy volunteers who underwent elective Cesarean section delivery.[6] In some mice, saline (vehicle) or 1×10^6 hAECs was injected into the tail vein either 1.5 or 72 hours after induction of MCAO. In others, hAECs were injected at 1 and/or 14 days after photothrombotic stroke. In marmosets, saline or hAECs (5×10^6) was injected into a saphenous vein 1.5 hours after initiation of ischemia.

Poststroke Assessment of Injury

Timelines for all cohorts (Figure I in the online-only Data Supplement) and detailed descriptions of methods for assessment of injury are in the online-only Data Supplement.

Statistical Analysis

Data are presented as scatter plots combined with mean±SEM, with the exception of neurological deficit scores (scatter plot with median). Analyses were performed using GraphPad Prism (San Diego, CA; v6.0). Between-group comparisons were made using 1-way ANOVA or Student unpaired *t* test. If differences were detected by ANOVA, individual groups were compared by Newman–Keuls or Tukey multiple comparison test. Neurological deficit scores were compared using a Mann–Whitney or Kruskal–Wallis test followed by Dunn test. Survival was analyzed using a log-rank test. Two independent variables were compared using a 2-way ANOVA, followed by either Bonferroni or Tukey test. Statistical significance was accepted if $P<0.05$.

Results

Characterization of hAECs

Primary hAEC isolates were gated positive for epithelial cell marker epithelial cell adhesion molecule (EpCAM) and negative for mesenchymal stromal markers CD90 and CD105 (Figure IIA in the online-only Data Supplement). $EpCAM^+CD90^-CD105^-$ cells were further gated for stem cell and stromal markers. Primary hAECs were >95% negative for CD146, STRO-1, and CD44 and >90% positive for SSEA-4, CD29, and CD73 (Figure IIB in the online-only Data Supplement).

Effects of hAECs After Transient MCAO in Young Male Mice

Acute hAEC Treatment Limits Functional Deficit and Infarct Volume

Male mice that received hAECs (10^6, IV) 1.5 hours after initiation of MCAO had less functional deficit at 24 and 72

hours than vehicle-treated mice. Specifically, hAEC-treated mice could grasp an elevated wire for approximately twice as long as vehicle-treated mice (Figure 1A), remove adhesive stickers from their forepaws quicker (Figure 1B), and had a lower median neurological deficit score (Figure 1C; P=0.06 at 72 hours). Infarct volume was reduced by ≥50% in hAECs-treated mice, as evidenced by thionin staining and sequential within-animal magnetic resonance analysis at 24, 48, and 72 hours (Figure 1D; Figure VIIC in the online-only Data Supplement)

Migration of hAECs to Brain and Spleen Is CXCR4 Dependent

hAECs labeled with carboxyfluorocein succinimidyl ester immediately before injection were detected in the ischemic hemisphere at 24 and 72 hours (Figure 2A and 2B) but not in the contralateral hemisphere (not shown) or in sham-operated mice (Figure 2A and 2B). hAECs were commonly localized to the infarct core (not shown) and spleen (Figure 2B). Few hAECs were in spleens of sham animals (Figure 2B), consistent with homing to multiple sites of injury and inflammation after stroke. Treatment of mice with CXCR4 antagonist, AMD3100, reduced hAECs by ≈70% in the poststroke brain (Figure 2C) accompanied by reduced grip strength and greater median neurological deficit score (Figure 2C), consistent with CXCR4/stromal cell derived factor 1–mediated tissue homing. Interestingly, hAECs were ineffective at reducing infarct volume or functional deficits in splenectomized animals (Figure 2D), suggesting that the spleen is required for hAECs to elicit neuroprotection.

hAECs Limit Stroke-Induced Cerebral Apoptosis and Inflammation

We assessed poststroke brain expression of apoptotic markers: cleaved caspase-3, annexin V, and cleaved caspase-8. Immunofluorescence with the neuronal marker, NeuN, and cleaved caspase-3 confirmed that most apoptotic cells were neurons (Figure 3A). Administration of hAECs resulted in fewer apoptotic cells at 24 and 72 hours (Figure 3A; Figure IIIA and IIIB in the online-only Data Supplement), an effect most evident in the infarct core (Figure 3A; Figure IIIA in the online-only Data Supplement). Expression of the

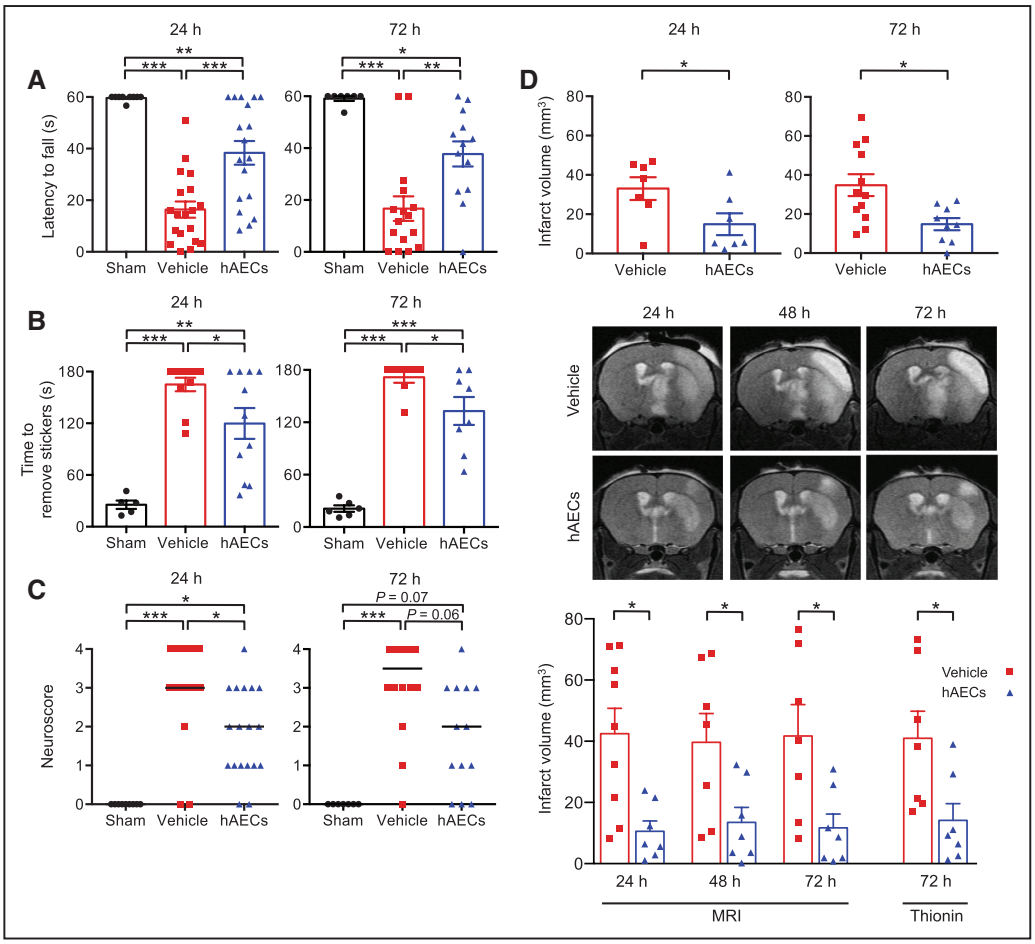

Figure 1. Acute administration of human amnion epithelial cells (hAECs) reduces functional deficits and infarct volume after stroke. Young male mice were subjected to either sham surgery or 30 minute transient middle cerebral artery occlusion and injected with vehicle or hAECs 1.5 hours later. Functional outcome and infarct volume were assessed at 24, 48, and 72 hours postsurgery. **A**, Latency to fall on hanging grip test (n=7–19). **B**, Latency to remove stickers on forepaws (n=5–11). **C**, Neurological deficit score (n=7–19). **D**, From top to bottom, Infarct volumes measured using thionin, representative images of magnetic resonance scans delineating infarct area at 24, 48, and 72 hours, infarct volumes measured by magnetic resonance imaging (MRI) at 24, 48, and 72 hours compared with 72 hours thionin (n=7–12). *P<0.05; **P<0.01; ***P<0.001, 1-way ANOVA and Tukey test (**A** and **B**), Kruskal–Wallis test and Dunn test (**C**), or Student unpaired t test (**D**). Data are mean±SEM (except neurological deficit scores presented as median).

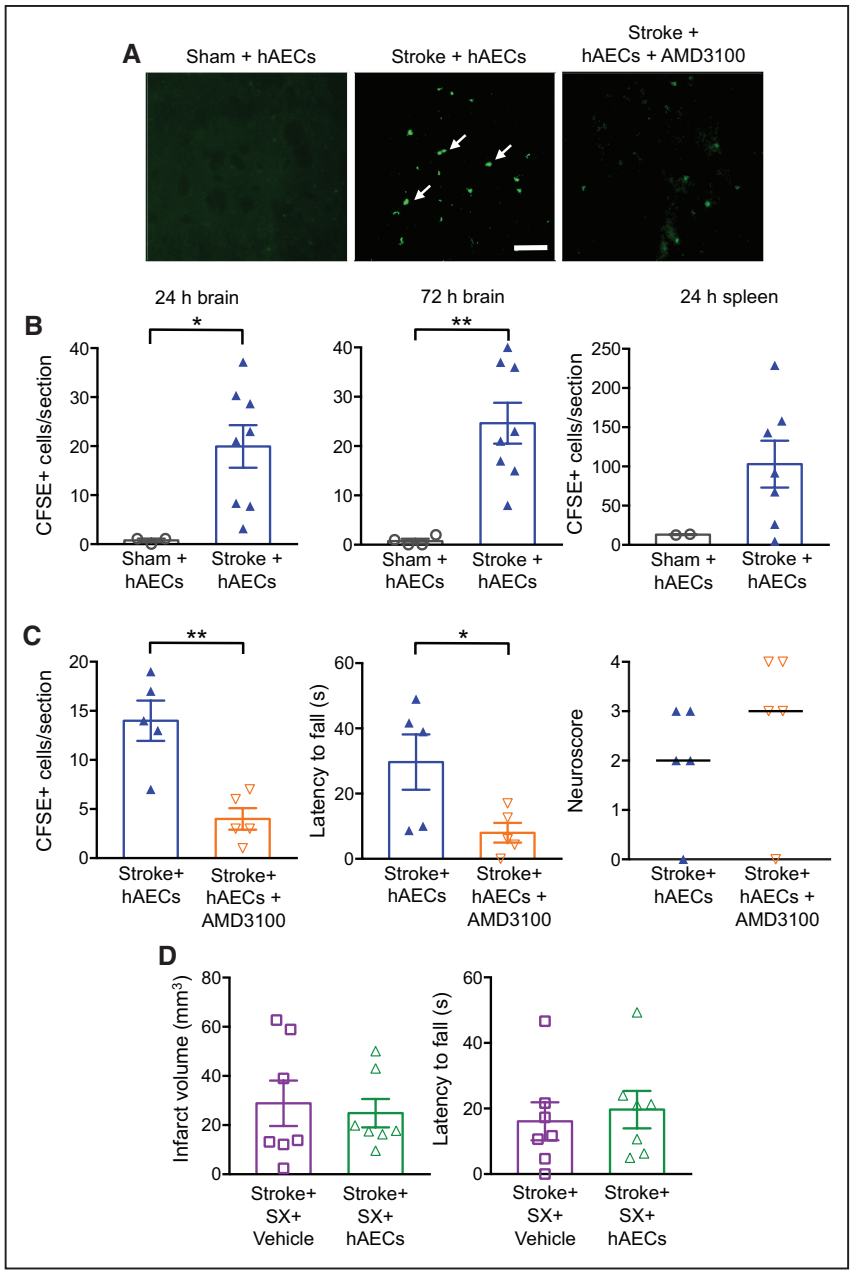

Figure 2. Intravenously administered human amnion epithelial cells (hAECs) migrate to the brain in a CXCR4-dependent manner after stroke and elicit neuroprotection in intact but not splenectomized (SX) mice. **A**, Representative images of (**B**) and (**C**). **B**, Young male mice were subjected to either sham surgery or 30 minute transient middle cerebral artery occlusion (MCAO), and carboxyfluorescein succinimidyl ester (CFSE)–labeled hAECs were injected 1.5 hours later. CFSE-labeled hAECs were counted in brain or spleen at 24 and 72 hours (n=2–8). **C**, Young male mice were subjected to 30 minute transient MCAO and injected with CFSE-labeled hAECs and vehicle or CXCR4 antagonist, AMD3100. From left to right, CFSE-labeled hAECs per brain section, latency to fall on hanging grip test, and neurological deficit scores (n=5). **D**, Young male SX mice were subjected to 60 minute transient MCAO and injected with either vehicle or hAECs at 1.5 hours. From left to right, Infarct volume and latency to fall on hanging grip test assessed at 24 hours poststroke (n=7). Scale bar indicates 100 μm. **P*<0.05; ***P*<0.01, Student unpaired *t* test. Data are mean±SEM (except neurological deficit scores, presented as median).

extrinsic apoptotic pathway mediator, cleaved caspase-8, was also reduced in hAEC-treated animals (Figure IIIC in the online-only Data Supplement). In a primary neuronal culture-based model of stroke, hAECs exerted no direct protection of neurons subjected to glucose-deprivation injury (Figure IIID in the online-only Data Supplement).

Inflammatory processes contribute to cerebral infarct formation and resultant neuronal death.[12–14] Because hAECs possess potent immunomodulatory properties,[9,15,16] we assessed their effect on immune cell infiltration into the ischemic hemisphere using immunohistochemistry (Figure 3B–3D) and flow cytometry (Figure IVA in the online-only Data Supplement). Increases in neutrophils, $CD3^+$ T cells, and macrophages at 24 and 72 hours were blunted in mice treated with hAECs (Figure 3B–3D; Figure IVA in the online-only Data Supplement). Moreover, the proportion of 3-nitrotyrosine–positive macrophages (consistent with a proinflammatory phenotype) was markedly reduced at 72 hours in hAECs-treated mice (Figure 3D). Flow cytometry confirmed these findings and revealed that ischemia-induced increases in B cells and $CD8^+$ T cells were also blunted by hAECs (Figure IVA in the online-only Data Supplement). Western blot analysis revealed that expression of the inflammasome protein, NOD-like receptor family pyrin domain–containing protein 3, was reduced in hAECs-treated animals at 24 hours (Figure IVB in the online-only Data Supplement).

hAECs Modulate Poststroke Immunosuppression

We tested whether treatment with hAECs affects stroke-induced systemic immunosuppression after early activation of the immune system. This phenomenon is an important cause of poststroke mortality and morbidity, the

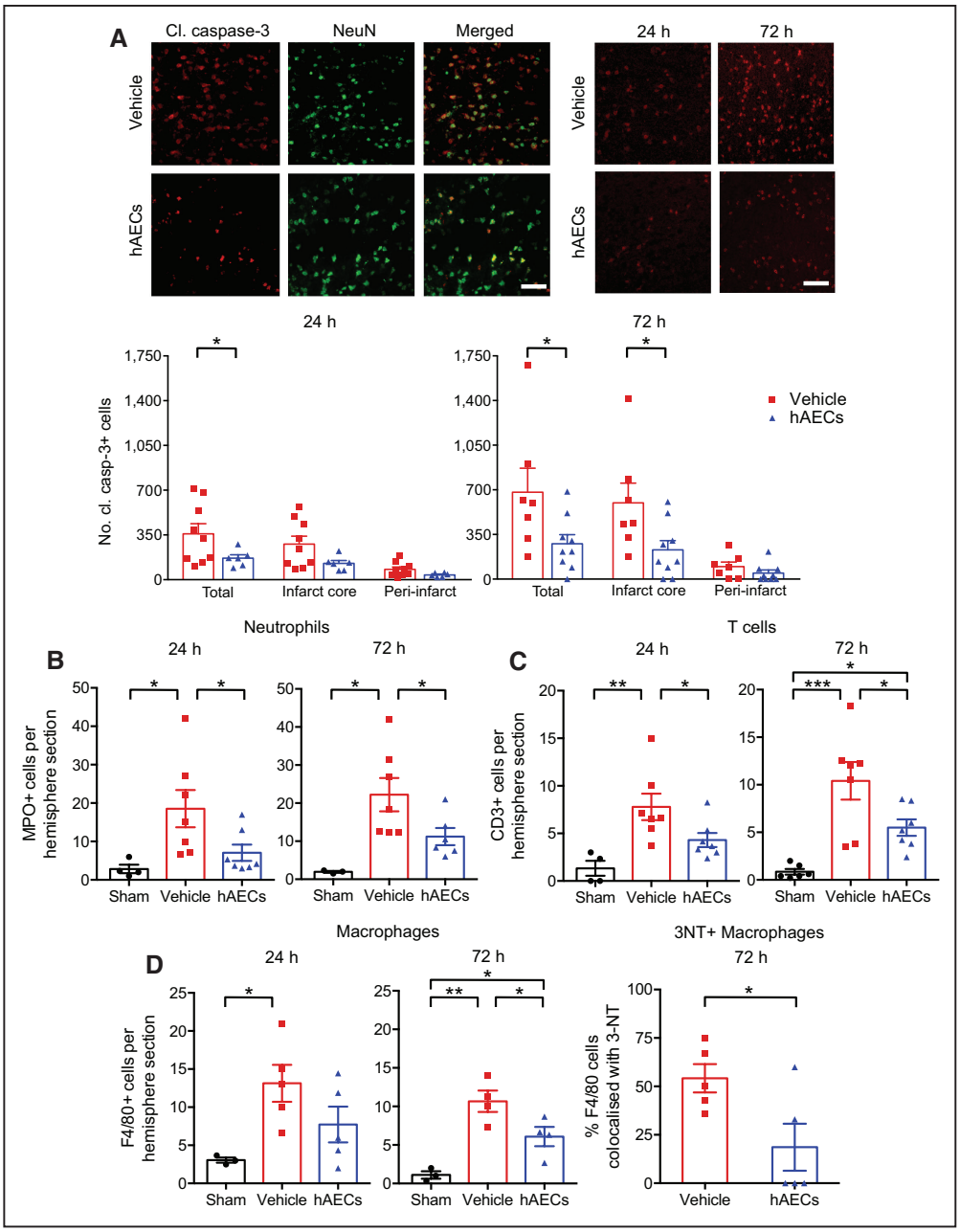

Figure 3. Acute administration of human amnion epithelial cells (hAECs) reduces cerebral apoptosis and inflammation after stroke. Young male mice were subjected to either sham surgery or 30 minute middle cerebral artery occlusion and injected with vehicle or hAECs 1.5 hours later. Apoptotic and immune cells were quantified in the brain at 24 and 72 hours postsurgery. **A**, Representative images showing colocalization of neuronal marker NeuN and cleaved caspase-3, and immunohistochemical analysis of immunoreactive cleaved caspase-3$^+$ (cl. casp 3$^+$) cells within the infarct core and peri-infarct region (n=6–9). Scale bars represent 100 μm. Immunohistochemistry was used to quantify: (**B**), myeloperoxidase (MPO)$^+$ cells (n=3–7), (**C**) CD3$^+$ cells (n=4–7), and (**D**), F4/80$^+$ cells (n=3–5) and 3-nitrotyrosine (3NT)$^+$ F4/80$^+$ cells (n=5) per ischemic/right hemisphere section. *P<0.05; **P<0.01; ***P<0.001, 2-way ANOVA (**A**), 1-way ANOVA followed by Newman–Keuls test (**B**–**D**), or Student unpaired t test (**D**). Data are mean±SEM.

major hallmarks of which include splenocyte apoptosis, splenic atrophy, loss of splenic and circulating leukocytes, and a weakened type 1 T helper cell response.[3] Indeed, the stroke-induced increase in apoptotic splenocytes evident by 24 hours preceded splenic atrophy at 72 hours, and these changes were blunted by hAECs (Figure VA and VB in the online-only Data Supplement). Flow cytometry confirmed that stroke resulted in fewer leukocytes in atrophied spleens and circulating blood (monocytes, neutrophils, B cells, CD4$^+$, and CD8$^+$ T cells) and that these reductions were attenuated by hAECs (Figure VC and VI in the online-only Data Supplement). Splenic expression of type 1 T helper cell (*Stat4*) and type 2 T helper cell (*Stat6*) transcription factors was elevated at 72 hours, an effect prevented by hAECs (Figure VIIA in the online-only Data Supplement). A similar profile was seen for the Th17 transcription factor, *Rorc* (Figure VIIA in the online-only Data Supplement). Aerobic bacterial infection of lungs at

72 hours was unaffected by hAECs (Figure VIIB in the online-only Data Supplement).

Delayed Treatment With hAECs Promotes Functional Recovery

We explored whether hAECs could impact functional recovery if administration was delayed for as long as 3 days—when infarct volume is fully formed in the mouse transient MCAO model (see Figure 1D). Mice administered hAECs at 3 days poststroke exhibited greater grip strength (Figure VIIIA in the online-only Data Supplement) and faster sticker removal at 7 to 14 days (Figure VIIIB in the online-only Data Supplement) and tended to have a greater 14-day survival rate than mice receiving saline at 3 days (Figure VIIIC in the online-only Data Supplement).

Effects of hAECs After Permanent MCAO in Young Male Mice

Acute Administration of hAECs Improves Outcome

Acute administration of hAECs modestly blunted the impact of cerebral ischemia with no reperfusion on several functional and histological indicators, resulting in faster sticker removal, a tendency for greater grip strength and lower neurological deficit, and ≈20% smaller infarcts (Figure 4A and 4B). There were also fewer CD3⁺ T cells, but not neutrophils, within the ischemic hemisphere of hAECs- than vehicle-treated mice (Figure 4C and 4D).

Effects of hAECs After Photothrombotic Stroke in Aged Female Mice

Delayed Treatment With hAECs Promotes Long-Term Functional Recovery

We then assessed the efficacy of hAECs injected at 1 and/or 14 days poststroke to reduce motor deficit over 8 weeks in a cohort of aged (20–22 months) female mice subjected to photothromobosis-induced ischemia of the primary motor cortex. Motor function was assessed by grid-walking and cylinder tests every 7 days. Mice treated with hAECs at either 1 day only or 1+14 days exhibited reduced preference for using their unaffected (left) rather than affected (right) forelimb in the cylinder test at 8 weeks compared with vehicle-treated mice (Figure 5A). This equated to an ≈40% improvement in limb function for 8 weeks as a result of hAECs treatment at 1-day poststroke, whereas no recovery occurred in vehicle-treated mice (Figure 5A). In the grid-walking test, ≈30% spontaneous recovery occurred in vehicle-treated mice by 8 weeks (Figure 5A). Similarly, mice treated with hAECs at 1±14 days made ≈40% fewer foot faults on their affected forepaw than vehicle-treated mice (Figure 5A). There was no apparent effect of hAECs on long-term motor function in either test if hAECs were administered only at 14 days (Figure 5A).

Delayed Administration of hAECs Stimulates Repair Mechanisms

A cohort of mice was studied to assess effects of hAECs administered 1-day poststroke on infarct development, peri-infarct

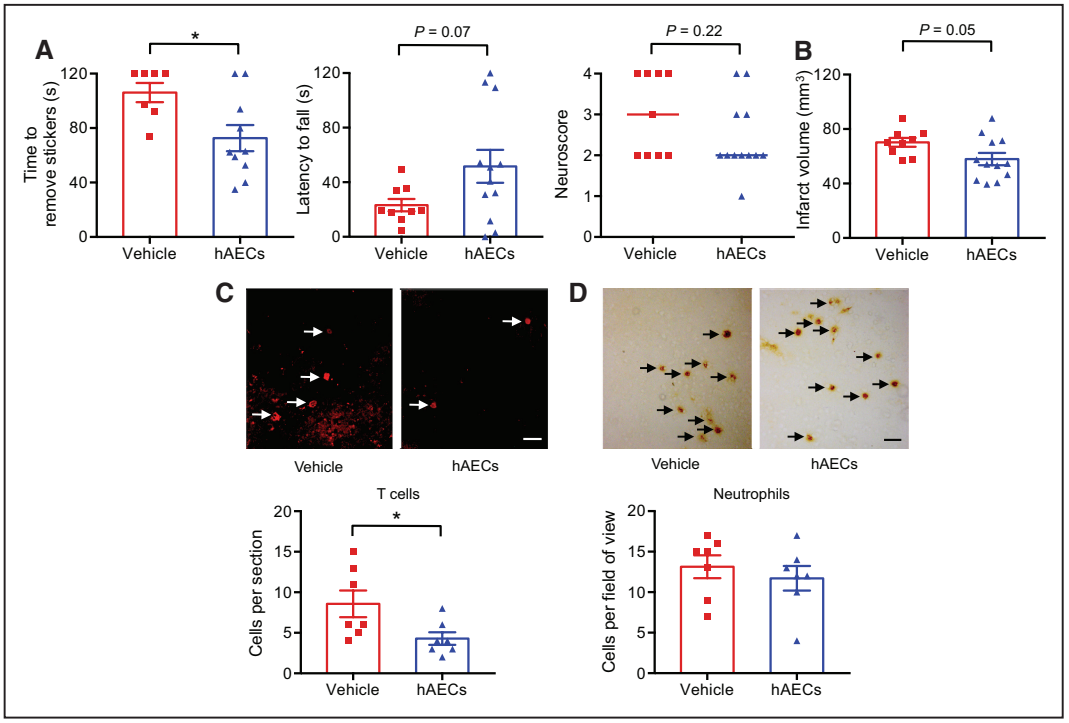

Figure 4. Efficacy of human amnion epithelial cells (hAECs) after permanent cerebral ischemia. Young male mice were subjected to permanent middle cerebral artery occlusion and injected with vehicle or hAECs at 1.5 hours. Functional outcome, infarct volumes, and brain immune cell numbers were assessed at 24 hours. **A**, From left to right, Latency to remove adhesive labels from forepaws, latency to fall in hanging grip test, and median neurological deficit score (n=7–12). **B**, Infarct volume (vehicle: n=9; hAECs: n=12). **C**, Immunohistochemical quantification of infiltrating CD3⁺ T cells per ischemic section (n=7/group). **D**, Immunohistochemical quantification of infiltrating myeloperoxidase (MPO)–positive neutrophils/field of view (n=7). Arrows indicate positive cells, scale bars represent 50 μm. *P<0.05, Student unpaired t test (**A**–**D**) except for neurological deficits scores which were compared using a Mann–Whitney test. Data are presented as mean±SEM except neurological deficit scores, presented as median.

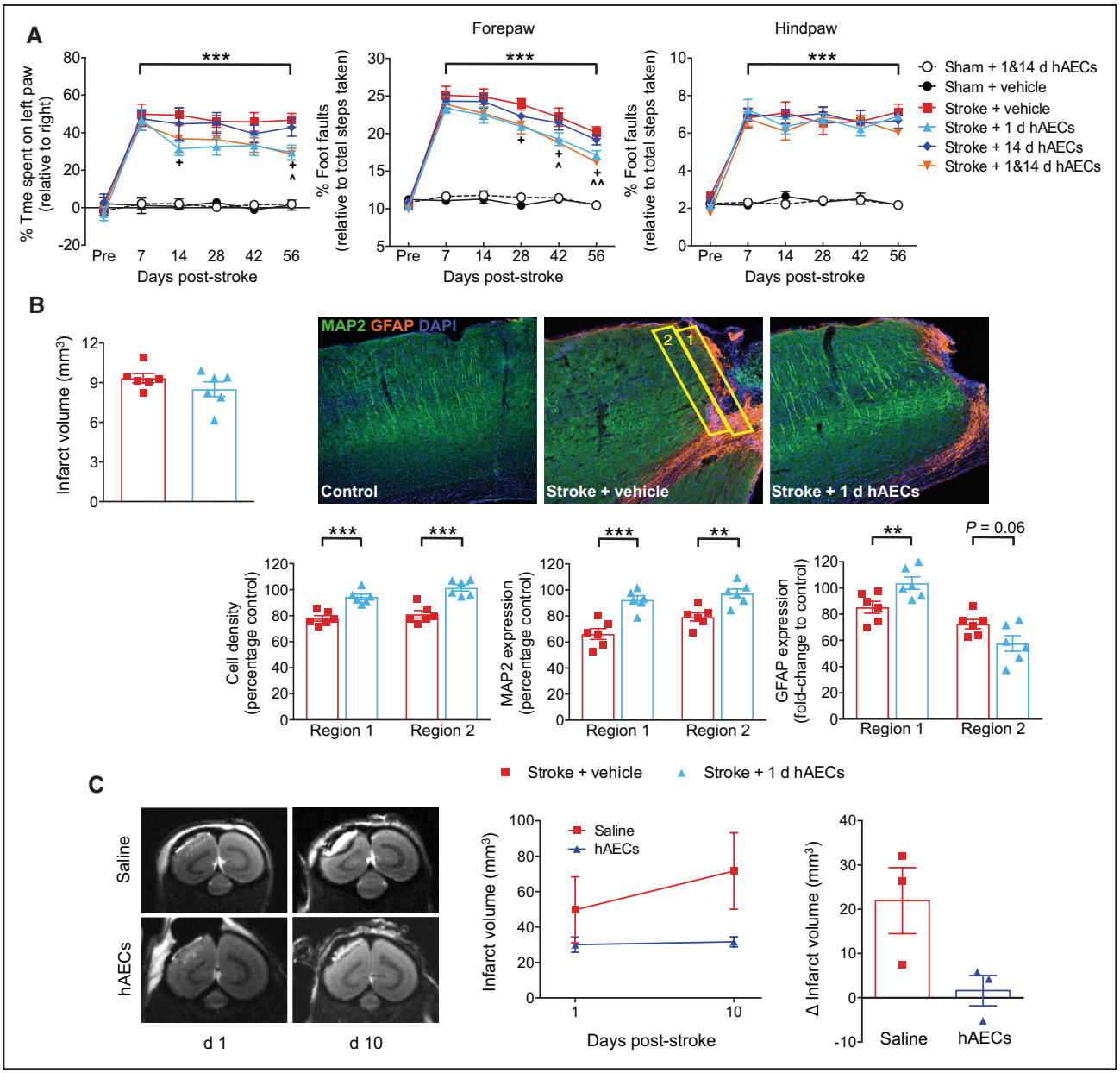

Figure 5. Administration of human amnion epithelial cells (hAECs) improves long-term outcome after stroke in aged female mice and marmosets. **A**, Mice were administered vehicle or hAECs at 1 or 14 days after sham surgery, or photothrombotic stroke and functional outcome were assessed for 56 days from left to right, Cylinder test assessing forepaw asymmetry, grid-walking test assessing forepaw and hindpaw deficits (n=7–8). ***P<0.001 (stroke vs sham), +P<0.05 (stroke+1 day hAECs vs stroke+vehicle), ^P<0.05 (stroke+1 and 14 days hAECs vs stroke+vehicle), ^^P<0.01 (stroke+1 and 14 days hAECs vs stroke+vehicle), 2-way ANOVA followed by Tukey' test. **B**, Mice were administered vehicle or hAECs 1 day postphotothrombosis and infarct volume and histological markers of peri-infarct plasticity were assessed at 7 days from top to bottom, left to right: Infarct volume at 7 days (n=6), immunohistochemical analysis of 4′,6-diamidino-2-phenylindole (DAPI), MAP2 (microtubule-associated protein-2), and GFAP (glial fibrillary acidic protein) of sham, vehicle- and hAECs-treated animals (n=6), representative images are shown above. Yellow boxes in the representative vehicle image show the regions of interest that were subjected to analysis. *P<0.05; **P<0.01; ***P<0.001, Student unpaired t test. **C**, Adult marmosets were subjected to endothelin-1–induced ischemia and injected with saline- or hAECs at 1.5 hours. Magnetic resonance (MR) imaging assessed infarct volumes at day 1 and day 10. From left to right, Representative MR scans delineating infarct area, mean infarct volume, and change in infarct volume from day 1 to day 10 in saline- and hAECs-treated marmosets (n=3; 2 males and 1 female/group). No statistical comparisons were made. All data are presented as mean±SEM.

plasticity, and/or the systemic inflammatory response at 7 or 56 days after photothrombotic stroke as potential mechanisms that impact long-term functional recovery. hAECs had no effect on infarct size at either 7 days (Figure 5B) or 56 days (Figure IXA in the online-only Data Supplement). We assessed changes in peri-infarct cortex plasticity by cell density, levels of microtubule-associated protein-2 (marker of neuronal dendrites), reactive astrogliosis (glial fibrillary acidic protein levels), and glutamic acid decarboxylase 67 (marker of inhibitory interneurons; Figure 5B; Figures IXB and X in the online-only Data Supplement). Administration of hAECs at 1 day resulted in a greater cell density and microtubule-associated

protein-2 immunoreactivity in both regions 1 and 2 at 7 days compared with vehicle-treated controls (Figure 5B). Reactive gliosis, as measured by glial fibrillary acidic protein expression, was increased in region 1 and tended to be decreased in region 2 at 7 days in animals that received hAECs compared with vehicle (Figure 5B). At 56 days, hAECs-treated animals had more reactive astrocytes within the glial scar despite a similar glial scar area in vehicle controls (Figure IXB in the online-only Data Supplement), and hAECs prevented the stroke-induced decrease in inhibitory interneurons (Figure X in the online-only Data Supplement). When assessing effects on the systemic immune response, we observed that hAECs reduced the expansion of myeloid cell compartments in bone marrow, spleen, and lymph nodes at 7 days (Figure XIA in the online-only Data Supplement) and prevented the reduction of circulating B cells and expansion of B cells in spleen and lymph nodes (Figure XIB in the online-only Data Supplement). hAECs also prevented the stroke-induced decrease in circulating T cells, without affecting T cell numbers in spleen or lymph nodes (Figure XIC in the online-only Data Supplement).

Effects of hAECs After Endothelin-1–Induced Stroke in Marmosets

hAECs Treatment Inhibits Infarct Expansion

We performed proof-of-concept studies in 6 marmosets injected intravenously with either saline or hAECs (5×10^6) 1.5 hours after initiation of cortical ischemia by injections of endothelin-1. Magnetic resonance analysis revealed infarct volume to be ≈70% and ≈125% larger on day 1 and day 10, respectively, in saline- versus hAECs-treated marmosets (Figure 5C). It was noteworthy that infarct volume expanded by >40% from day 1 to day 10 in saline-treated marmosets, whereas infarct expansion was largely arrested in hAECs-treated animals (Figure 5C).

Discussion

We have used 4 models of ischemic stroke in immunocompetent animals to assess the effects of hAECs on stroke outcomes. When injected intravenously after ischemia onset, hAECs migrate preferentially to the spleen and injured brain to limit apoptosis and inflammation and attenuate early brain infiltration of immune cells, progression of infarction, and systemic immunodepression to ultimately ameliorate functional deficits. When administration of hAECs was delayed by 1 to 3 days, long-term functional recovery could still be enhanced in young and aged mice of either sex, regardless of infarct size or whether early reperfusion had occurred. Moreover, proof-of-principle findings suggested that hAECs are effective at limiting infarct development in nonhuman primates.

Previous assessment of cell-based therapies in animal models of stroke have commonly used direct intracerebral administration of stem cells.[17–19] This invasive approach is unlikely to be practicable clinically for several reasons. First, intracerebral administration will likely require expensive imaging equipment and expertise not readily available in most centers. Intracerebral administration may itself cause further brain injury,[20] and such an approach does not likely target the systemic mechanisms that contribute to impaired outcomes after stroke.[2,3] More recent studies have demonstrated beneficial effects from intravenous administration of stem cells[21–23] although immunologic rejection, tumorigenesis, and ethical and logistical obstacles may limit the practicality of their use. By contrast, because these limitations do not seem to apply to hAECs,[5] we explored their therapeutic utility when administered systemically after stroke.

We found that hAECs migrated to the infarct core but not contralateral hemisphere or into brains of sham-operated animals, indicating that these cells homed to damaged areas of brain. As reported for other stem cell lineages,[4,13] hAECs seem to migrate to the brain via stromal cell derived factor 1–CXCR4 signaling. We observed fewer apoptotic cells within the hAECs-containing infarct core; however, because hAECs did not directly protect neurons subjected to ischemia-like injury in vitro, the neuroprotection achieved in vivo is likely to have involved the coordination of complex mechanisms involving multiple cell types. We found that a substantial proportion of intravenously injected hAECs migrated to the spleen after stroke and that hAECs had reduced efficacy in splenectomized animals, suggesting that the spleen is required for full neuroprotection by hAECs. This is analogous to the observation that hAECs require functional macrophages and T cells to exert protective and reparative effects in a murine model of idiopathic pulmonary fibrosis.[15,24]

Likely mechanisms by which hAECs elicit neuroprotection and functional recovery when given up to 3 days poststroke are via modulation of inflammatory responses during the acute (hours) and subacute (days) phases of cerebral ischemia.[12] hAECs reduce inflammation in other disease settings[9,15] by inhibiting neutrophil and macrophage migration, promoting M2 (as opposed to M1) polarization of macrophages,[16] reducing proliferation of activated T and B cells, and inducing regulatory T cells.[15,25] We observed similar effects of hAECs in our stroke models, with profoundly reduced infiltration of leukocytes into the injured brain after either transient or permanent ischemia. Of note, there was a ≈75% reduction in 3-nitrotyrosine–positive macrophages, reflecting M1-polarized cells that exacerbate inflammation and promote neuronal death.[14]

We examined effects of hAECs on peripheral immune function, which is thought to be augmented for up to 24 hours after stroke and followed by a profound immunosuppression. This delayed phase of systemic immune system suppression may render patients with stroke especially vulnerable to infections.[3] In addition to modulating the initial proinflammatory response to stroke, hAECs therapy also blunted several features of systemic immunosuppression by 72 hours, including apoptotic loss of splenocytes, splenic atrophy, and leukopenia.

We assessed the potential of hAECs to modulate repair processes and facilitate functional recovery when administered at delayed time points. We observed greater hanging grip strength and faster adhesive removal over 1 to 2 weeks compared with saline when hAECs were injected 3 days after stroke. Because the majority of clinical strokes occur in people of advancing age (ie, >65 years), it is important that preclinical stroke research evaluates potential therapies in aged animals and in both sexes. Indeed, we found that aged female mice receiving hAECs at 1 day after stroke exhibited a 30% to 40% greater

long-term motor recovery over 8 weeks compared with mice receiving vehicle. No benefit was seen from an additional or alternative injection of hAECs at 14 days. To explore potential mechanisms of improved recovery, we assessed changes in reactive astrogliosis, dendritic plasticity, and GABA signaling. Treatment with hAECs resulted in greater expression of glial fibrillary acidic protein at the site of the lesion border but decreased the spread of reactive astrogliosis into neighboring tissue regions. Furthermore, stroke-induced decreases in peri-infarct microtubule-associated protein-2 and glutamic acid decarboxylase 67 were reversed by hAECs. These changes in peri-infarct cortex plasticity occurred in association with a modulated systemic inflammatory response, whereby hAECs reduced the stroke-induced increase in myeloid and B cells within bone marrow, spleen, and lymph nodes. Our findings indicate that subacute (1–3 days) administration of hAECs can substantially modify pathological mechanisms that lead to long-term functional impairment after stroke, indicating a powerful capacity for repair and recovery by hAECs when given within a wide therapeutic window.

A common finding between our acute and delayed administration protocols was that hAECs were able to modify the poststroke immune response. It is conceivable that acute administration of hAECs would be necessary to sequester inflammation, which can directly contribute to poststroke brain injury. However, modulating the immune response even after brain injury is fully established would still likely be of benefit. For example, one study reported that B cells infiltrate the brain weeks after a stroke and lead to delayed cognitive impairment.[26] Furthermore, hAECs can promote T regulatory cell expansion and M2 macrophage polarization,[15,16] which may aid in brain repair processes. Therefore, inhibiting delayed immune cell infiltration into the brain and promoting the development of reparative immune cell subsets could lead to a favorable long-term outcome poststroke.

Last, because there are several important physiological and anatomic differences between brains of lower-order species such as rodents and those of humans, we also wished to assess the effect of hAECs in a small cohort of New World marmoset monkeys, which share similarities to humans about brain anatomy.[27] We found that the degree of neuroprotection achieved by intravenous administration of hAECs to a small number of marmosets after stroke was comparable or greater in magnitude to that observed in mice and that hAECs therapy effectively prevented the infarct expansion that occurs between day 1 and day 10 in that species.

From a translational perspective, it has been known for >30 years that hAECs are safe to transplant to humans.[28] Indeed, amnion cells or strips of amnion membrane have long been used to reduce scarring and promote healing in burn victims or after corneal surgery.[29,30] Therefore, it is conceivable that hAECs could also be safely administered to patients with stroke. We do not currently know whether poststroke hAECs engraftment (migration and survival) is similar for mice and marmosets. It is noteworthy that we chose to not routinely use a cell-based control. This was in keeping with our original intent, which was to report on the impact of hAEC therapy on stroke-related brain injury, and as such our control for hAEC delivery was simply the absence of hAECs (ie, saline/vehicle). In pilot experiments, we did assess the effect of intravenous injection of mouse embryonic stem cells on stroke outcome and found them to be ineffective at reducing infarct volume or associated functional deficits (Figure XIIA–XIIC in the online-only Data Supplement). These data are compatible with our conclusion that the protective effects of poststroke injection of hAECs were inherent to that cell type and not because of administration of cellular content.

In summary, we have shown that hAECs administered systemically to mice up to 3 days after ischemic stroke can reduce brain injury, inflammation, and both short- and long-term functional deficits in young adult and aged animals of both sexes. Our study includes proof-of-principle evidence that poststroke administration of hAECs leads to neuroprotection in nonhuman primates. Overall, these findings suggest that hAECs could be a viable and effective clinical stroke therapy.

Sources of Funding

These studies were supported by a Grant-In-Aid (G11M5907) from the Heart Foundation of Australia. We acknowledge support from a Contributing to Australian Scholarship and Science Foundation grant (Dr Broughton), Monash Strategic Grant (Dr Broughton), Monash Faculty Postgraduate Scholarship (Dr Evans), Australian Postgraduate Awards (Drs Chu, Chan, and Dinh), National Stroke Foundation Honours Grant (C.V. Gardiner-Mann), Monash Postgraduate Research Scholarship (Dr Brait), New Zealand Lottery Health Postdoctoral Fellowship (Dr Neumann), Australian Research Council Future Fellowship (Dr Arumugam), National Health and Medical Research Council of Australia Senior Research Fellowships (Drs Drummond and Sobey), National Health and Medical Research Council of Australia Project Grant (Drs Wallace and Lim), New Zealand Neurological Foundation and Royal Society of New Zealand Project Grant (Dr Clarkson), Maurice and Phyllis Paykel Trust (Dr Clarkson), and Victorian Government's Operational Infrastructure Support Program (Drs Wallace and Lim).

Disclosures

None.

References

1. Del Zoppo GJ, Saver JL, Jauch EC, Adams HP Jr; American Heart Association Stroke Council. Expansion of the time window for treatment of acute ischemic stroke with intravenous tissue plasminogen activator: a science advisory from the American Heart Association/American Stroke Association. *Stroke*. 2009;40:2945–2948. doi: 10.1161/STROKEAHA.109.192535.
2. Dirnagl U, Endres M. Found in translation: preclinical stroke research predicts human pathophysiology, clinical phenotypes, and therapeutic outcomes. *Stroke*. 2014;45:1510–1518. doi: 10.1161/STROKEAHA.113.004075.
3. Shim R, Wong CH. Ischemia, immunosuppression and infection–tackling the predicaments of post-stroke complications. *Int J Mol Sci*. 2016;17:E64.
4. Zhang J, Chopp M. Cell-based therapy for ischemic stroke. *Expert Opin Biol Ther*. 2013;13:1229–1240. doi: 10.1517/14712598.2013.804507.
5. Broughton BR, Lim R, Arumugam TV, Drummond GR, Wallace EM, Sobey CG. Post-stroke inflammation and the potential efficacy of novel stem cell therapies: focus on amnion epithelial cells. *Front Cell Neurosci*. 2012;6:66. doi: 10.3389/fncel.2012.00066.
6. Murphy S, Rosli S, Acharya R, Mathias L, Lim R, Wallace E, et al. Amnion epithelial cell isolation and characterization for clinical use. *Curr Protoc Stem Cell Biol*. 2010;Chapter 1:Unit 1E.6. doi: 10.1002/9780470151808.sc01e06s13.
7. Miki T, Lehmann T, Cai H, Stolz DB, Strom SC. Stem cell characteristics of amniotic epithelial cells. *Stem Cells*. 2005;23:1549–1559. doi: 10.1634/stemcells.2004-0357.

8. Kakishita K, Elwan MA, Nakao N, Itakura T, Sakuragawa N. Human amniotic epithelial cells produce dopamine and survive after implantation into the striatum of a rat model of Parkinson's disease: a potential source of donor for transplantation therapy. *Exp Neurol*. 2000;165:27–34. doi: 10.1006/exnr.2000.7449.
9. McDonald CA, Payne NL, Sun G, Moussa L, Siatskas C, Lim R, et al. Immunosuppressive potential of human amnion epithelial cells in the treatment of experimental autoimmune encephalomyelitis. *J Neuroinflammation*. 2015;12:112. doi: 10.1186/s12974-015-0322-8.
10. Stroke Therapy Academic Industry Roundtable (STAIR). Recommendations for standards regarding preclinical neuroprotective and restorative drug development. *Stroke*. 1999;30:2752–2758. doi: 10.1161/01.STR.30.12.2752.
11. Savitz SI, Chopp M, Deans R, Carmichael T, Phinney D, Wechsler L; STEPS Participants. Stem Cell Therapy as an Emerging Paradigm for Stroke (STEPS) II. *Stroke*. 2011;42:825–829. doi: 10.1161/STROKEAHA.110.601914.
12. Anrather J, Iadecola C. Inflammation and stroke: an overview. *Neurotherapeutics*. 2016;13:661–670. doi: 10.1007/s13311-016-0483-x.
13. Stonesifer C, Corey S, Ghanekar S, Diamandis Z, Acosta SA, Borlongan CV. Stem cell therapy for abrogating stroke-induced neuroinflammation and relevant secondary cell death mechanisms. *Prog Neurobiol*. 2017;158:94–131. doi: 10.1016/j.pneurobio.2017.07.004.
14. Benakis C, Garcia-Bonilla L, Iadecola C, Anrather J. The role of microglia and myeloid immune cells in acute cerebral ischemia. *Front Cell Neurosci*. 2014;8:461. doi: 10.3389/fncel.2014.00461.
15. Tan JL, Chan ST, Lo CY, Deane JA, McDonald CA, Bernard CC, et al. Amnion cell-mediated immune modulation following bleomycin challenge: controlling the regulatory T cell response. *Stem Cell Res Ther*. 2015;6:8. doi: 10.1186/scrt542.
16. Tan JL, Chan ST, Wallace EM, Lim R. Human amnion epithelial cells mediate lung repair by directly modulating macrophage recruitment and polarization. *Cell Transplant*. 2014;23:319–328. doi: 10.3727/096368912X661409.
17. Zhang P, Li J, Liu Y, Chen X, Kang Q, Zhao J, et al. Human neural stem cell transplantation attenuates apoptosis and improves neurological functions after cerebral ischemia in rats. *Acta Anaesthesiol Scand*. 2009;53:1184–1191. doi: 10.1111/j.1399-6576.2009.02024.x.
18. Lin YC, Ko TL, Shih YH, Lin MY, Fu TW, Hsiao HS, et al. Human umbilical mesenchymal stem cells promote recovery after ischemic stroke. *Stroke*. 2011;42:2045–2053. doi: 10.1161/STROKEAHA.110.603621.
19. Liu T, Wu J, Huang Q, Hou Y, Jiang Z, Zang S, et al. Human amniotic epithelial cells ameliorate behavioral dysfunction and reduce infarct size in the rat middle cerebral artery occlusion model. *Shock*. 2008;29:603–611. doi: 10.1097/SHK.0b013e318157e845.
20. McCluskey L, Campbell S, Anthony D, Allan SM. Inflammatory responses in the rat brain in response to different methods of intra-cerebral administration. *J Neuroimmunol*. 2008;194:27–33. doi: 10.1016/j.jneuroim.2007.11.009.
21. Acosta SA, Tajiri N, Hoover J, Kaneko Y, Borlongan CV. Intravenous bone marrow stem cell grafts preferentially migrate to spleen and abrogate chronic inflammation in stroke. *Stroke*. 2015;46:2616–2627. doi: 10.1161/STROKEAHA.115.009854.
22. Golden JE, Shahaduzzaman M, Wabnitz A, Green S, Womble TA, Sanberg PR, et al. Human umbilical cord blood cells alter blood and spleen cell populations after stroke. *Transl Stroke Res*. 2012;3:491–499. doi: 10.1007/s12975-012-0208-3.
23. Vendrame M, Gemma C, Pennypacker KR, Bickford PC, Davis Sanberg C, Sanberg PR, et al. Cord blood rescues stroke-induced changes in splenocyte phenotype and function. *Exp Neurol*. 2006;199:191–200. doi: 10.1016/j.expneurol.2006.03.017.
24. Murphy SV, Shiyun SC, Tan JL, Chan S, Jenkin G, Wallace EM, et al. Human amnion epithelial cells do not abrogate pulmonary fibrosis in mice with impaired macrophage function. *Cell Transplant*. 2012;21:1477–1492. doi: 10.3727/096368911X601028.
25. McDonald C, Siatskas C,Bernard CCA. The emergence of amnion epithelial stem cells for the treatment of multiple sclerosis. *Inflamm Regen*. 2011;31:256–271.
26. Doyle KP, Quach LN, Solé M, Axtell RC, Nguyen TV, Soler-Llavina GJ, et al. B-lymphocyte-mediated delayed cognitive impairment following stroke. *J Neurosci*. 2015;35:2133–2145. doi: 10.1523/JNEUROSCI.4098-14.2015.
27. Teo L, Bourne JA. A reproducible and translatable model of focal ischemia in the visual cortex of infant and adult marmoset monkeys. *Brain Pathol*. 2014;24:459–474. doi: 10.1111/bpa.12129.
28. Akle CA, Adinolfi M, Welsh KI, Leibowitz S, McColl I. Immunogenicity of human amniotic epithelial cells after transplantation into volunteers. *Lancet*. 1981;2:1003–1005.
29. Payne WG, Wachtel TL, Smith CA, Uberti MG, Ko F, Robson MC. Effect of amnion-derived cellular cytokine solution on healing of experimental partial-thickness burns. *World J Surg*. 2010;34:1663–1668. doi: 10.1007/s00268-010-0420-9.
30. Kheirkhah A, Johnson DA, Paranjpe DR, Raju VK, Casas V, Tseng SC. Temporary sutureless amniotic membrane patch for acute alkaline burns. *Arch Ophthalmol*. 2008;126:1059–1066. doi: 10.1001/archopht.126.8.1059.

Acute or Delayed Systemic Administration of Human Amnion Epithelial Cells Improves Outcomes in Experimental Stroke

Megan A. Evans, Rebecca Lim, Hyun Ah Kim, Hannah X. Chu, Chantelle V. Gardiner-Mann, Kimberly W.E. Taylor, Christopher T. Chan, Vanessa H. Brait, Seyoung Lee, Quynh Nhu Dinh, Antony Vinh, Thanh G. Phan, Velandai K. Srikanth, Henry Ma, Thiruma V. Arumugam, David Y. Fann, Luting Poh, Cameron P.J. Hunt, Colin W. Pouton, John M. Haynes, Stavros Selemidis, William Kwan, Leon Teo, James A. Bourne, Silke Neumann, Sarah Young, Emma K. Gowing, Grant R. Drummond, Andrew N. Clarkson, Euan M. Wallace, Christopher G. Sobey and Brad R.S. Broughton

Stroke. 2018;49:700-709; originally published online January 30, 2018;
doi: 10.1161/STROKEAHA.117.019136
Stroke is published by the American Heart Association, 7272 Greenville Avenue, Dallas, TX 75231

Print ISSN: 0039-2499. Online ISSN: 1524-4628

SUPPLEMENTAL MATERIAL

Acute or delayed systemic administration of human amnion epithelial cells improves outcomes in experimental stroke

Megan A Evans, PhD, Rebecca Lim, PhD, Hyun Ah Kim, PhD, Hannah X Chu, PhD, Chantelle V Gardiner-Mann, BSc(Hons), Kimberly WE Taylor, BSc(Hons), Christopher T Chan, PhD, Vanessa H Brait, PhD, Seyoung Lee, PhD, Quynh Nhu Dinh, PhD, Antony Vinh, PhD, Thanh G Phan, MD PhD, Velandai K Srikanth, MD PhD, Henry Ma MD, Thiruma V Arumugam, PhD, David Y Fann, PhD, Poh Luting, BSc(Hons), Cameron PJ Hunt, PhD, Colin W Pouton, PhD, John M. Haynes, PhD, Stavros Selemidis, PhD, William Kwan, BBiomedSc(Hons), Leon Teo, PhD, James A Bourne, PhD, Silke Neumann, PhD, Sarah Young, PhD, Emma K Gowing, BSc(Hons), Grant R Drummond, PhD, Andrew N Clarkson, PhD, Euan M Wallace, MD, Christopher G Sobey*, PhD, Brad RS Broughton*, PhD.

Study design

The purpose of this study was to test the efficacy of systemically delivered hAECs in established animal models of ischemic stroke. These studies were performed in support of several STAIRs[1] and STEPs[2] recommendations, as we utilized models of permanent and transient cerebral ischemia, animals of both sexes, aged animals and non-human primates. We also assessed different timepoints at which hAECs could be delivered after stroke. Sample sizes were selected based on previous published work[3-5]. All animals were assigned to an experimental group by a coin toss or equivalent randomization protocol and the investigator performing the surgical procedure or data analysis was, wherever possible, blinded to the treatment group by the use of coding. See figure I for experimental timeline outlining the models of stroke that were used in this study.

Animals

These studies were approved by Monash University and University of Otago Animal Ethics Committees and performed in accordance with the National Health and Medical Research Council of Australia guidelines for the care and use of animals in research. A total of 326 male C57Bl6 mice (7-14 week-old; 21-33 g), 68 aged female C57Bl6 mice (20-22 months-old; 30-33 g) and 6 timed-pregnant female C57Bl6 mice were used for this study. Mice were housed in specific pathogen free cages and had free access to water and food pellets. Mice were excluded from the study if during the surgical procedure to induce middle cerebral artery occlusion >0.2 ml of blood was lost, or the occluding clamp on the common carotid artery was in place for ≥7 min, or if death occurred prior to the designated time for euthanasia. We also studied 6 adult New World marmoset monkeys (*Callithrix jacchus*; 3-5 years; 2 female, 4 male). Sex was not a criterion in the selection of marmosets, and no siblings were used.

Middle cerebral artery occlusion model of stroke

Mice underwent either sham surgery or focal cerebral ischemia as previously described[3, 6]. Ischemia was produced in anesthetized mice (ketamine: 80 mg/kg plus xylazine: 10 mg/kg i.p.) by occlusion of the right middle cerebral artery (MCA) using a 6.0 silicone-coated monofilament (Doccol Corporation). Rectal temperature was monitored and maintained at 37.0±0.5 °C. MCA occlusion (MCAO) was sustained for either 30 or 60 min, and the filament then retracted to allow reperfusion. Both successful occlusion (>70 % reduction in cerebral blood flow; CBF) and reperfusion (>80 % return of CBF to pre-ischemic levels) was confirmed by transcranial laser-Doppler flowmetry (PeriMed). In some experiments the filament was not retracted in order to induce permanent MCAO. Sham-operated mice were anesthetized and the right carotid bifurcation exposed, but no filament was inserted. Neck and head wounds were then closed, covered with Betadine® (Sanofi) and spray dressing, and mice were returned to their cages after regaining consciousness. Immediately after surgery, all animals received 1 ml of sterile saline (s.c.). Close monitoring was performed after surgery until the time of euthanasia.

Photothromotic model of cortical stroke

Focal stroke of the primary motor cortex (M1) was induced by photothrombosis in aged (20-22 month old) female C57BL6 mice as previously described[7, 8]. Under isoflurane anesthesia (2-2.5 % in O_2) mice were placed in a stereotaxic apparatus, the skull was exposed through a midline incision, cleared of connective tissue and dried. A cold light source (KL1500 LCD, Zeiss) attached to a 40x objective and giving a 2 mm diameter of illumination was positioned 1.5 mm lateral from the bregma, and 0.2 ml of Rose Bengal (Sigma; 10 mg/ml in normal saline, i.p.) was administered. After 5 min the brain was illuminated through the intact skull for 15 min. Head wounds were then closed and mice were allowed to regain consciousness.

Endothelin-1 (ET-1) model of cortical stroke in non-human primates

Ischemic stroke was produced in the left primary visual cortex (V1) of adult marmosets by targeted intracortical injections of ET-1 proximal to the calcarine artery, which resulted in transient arterial occlusion, as we have previously reported[9]. Anesthesia was induced with alfaxalone (8 mg/kg i.m.) and maintained with inspired isoflurane (~2 %). Physiological conditions were continuously monitored using a pulse oximeter and temperature probe and kept within strict parameters. Intracortical injections were performed in doses of 0.1 µl/30 s pulse at 30 s intervals to administer ~0.7 µl of endothelin-1 (ET-1) (1 µg/µl; Sigma-Aldrich). Post-injection, the needle remained *in situ* for a further 2 min before withdrawal. Intracortical ET-1 injections surrounding the calcarine artery were performed over ≤7 sites. To determine the extent of ET-1 induced ischemic injury, continuous video monitoring of cortical surface was performed throughout. Injections of ET-1 caused sustained calcarine vasoconstriction, accompanied by vascular stasis and collapse immediately downstream of occlusion sites with visible pallor of the surrounding cortical surface. Reperfusion usually occurs within 4 h of vessel occlusion in this model[9]. At 1.5 h following the initiation of ET-1-induced ischemia, saline or hAECS ($5x10^6$) was injected in 1 mL into the right saphenous vein. There were 2 males and 1 female in each treatment group. The limited behavioral consequences associated with these discrete lesions of V1, scotoma/'blindspot' in the contralateral visual field, still enabled the animals to ambulate and feed normally after recovery from anesthesia without significant human intervention[9]. Immediately after surgery, animals were placed in a recovery cage for

approximately 3 h for close monitoring. All animals were monitored twice daily until the time of euthanasia.

Comparison of mouse and marmoset models of cortical stroke.

RIGOR guidelines recommend multiple species and models of injury to demonstrate the efficacy of an experimental stroke treatment[10]. Small cortical infarction has been reported to occur in 22.8% of patients with acute ischemic stroke[11]. Here, both models of cortical stroke (i.e. photothrombosis in mice; endothelin-1 in marmosets) produce an infarct restricted to ~5% of the cortex, which is comparable to 5-15% in most human strokes[12, 13]. In addition, mice, marmosets and humans develop similar comparative post-stroke pathologies, except that some cellular events occur more quickly in mice, such as astrogliosis which corresponds to the formation of the glial scar. For example, MRI fogging, which coincides with the peak of astrogliosis, appears at 3-9 d in mouse[14, 15], at 14-21d in marmosets[9], and at 10-28 d in humans[16, 17]. Nevertheless, by 24 h in both mice and marmosets, neuronal necrosis in the infarct core is mostly completed, BBB breakdown is evident and onset of neuronal apoptosis in the peri-infarct has begun. Further, the mouse photothrombosis model has a small reperfusion component[18] and, whereas the marmoset endothelin-1 model has full large vessel reperfusion within 4 h, it is currently unclear if or when effective reperfusion of the microvasculature occurs. Overall, we suggest that these two models approximate a similar clinical scenario of cortical stroke.

Splenectomy

For some experiments, spleens of 6-8 week-old male mice were removed surgically under aseptic conditions 2 w prior to MCAO. Mice were anesthetized with a mixture of ketamine (80 mg/kg) and xylazine (10 mg/kg). A 10 mm incision was made in the left flank, caudal to the last rib, to expose the spleen. The splenic arteries and efferent veins were then cauterized, taking care not to disturb underlying pancreatic tissue. The spleen was then removed from the abdominal cavity and the peritoneum and skin were closed separately using 6.0 nylon sutures. Mice were given an injection of Atipamezole HCl (antisedan; 100 mg/kg i.p.) to reverse anesthesia and were allowed to recover before being returned to their cages. Animals were monitored daily for 2 w following surgery.

hAEC isolation, labeling, and injection

hAECs were isolated from term placentae donated by healthy volunteers who underwent elective Cesarean section delivery; the procedures have previously been described in detail[19]. Cells were thawed and cultured for a minimum of 12 h in Dulbecco's Modified Eagle Medium: Nutrient Mixture F-12 (DMEM/F12; Life Technologies) containing 10 % fetal bovine serum (FBS; Sigma). Cell viability was assessed by trypan blue exclusion and isolates with a minimum of 80 % viability were used. In some experiments, first-passage hAECs were labeled passively with carboxyfluorescein succinimidyl ester (CFSE; Abcam) prior to injection to enable identification in tissues, and were suspended in sterile saline at $5x10^6$/ml. Saline (vehicle) or $1x10^6$ hAECs was injected into the tail vein of mice. For acute administration, hAECs were injected 1.5 h after the induction of MCAO. For delayed administration in young male mice, hAECs were injected 72 h post-stroke. For studies in aged female mice, hAECs were injected at 1 d and/or 14 d post-stroke. Where tail vein injections were not possible due to the advanced age of these mice, combined tail vein (usually one-third) and subcutaneous (two-thirds) injections were given.

Characterization of hAECs by flow cytometry

Primary hAECs were stained with antibodies and analyzed by flow cytometry accordingly. hAECs at a density of 1 x 10^6/ml were suspended in FACS Buffer (HBSS + 10 % FBS) and stained for EpCAM-PE (1:50), CD105-PE-Cy7 (1:100), CD146-BV421 (1:100), STRO-1-AF647 (1:100), CD44-BV510 (1:100), SSEA-4-FITC (1:100), CD29-AF700 (1:200), CD73-APC Cy7 (1:100) for 30 min at 4°C in the dark. Cells were then washed and acquired using the LSRII flow cytometer (BD Biosciences) and analyzed using the BD FACSDiva Software (BD Biosciences).

Administration of AMD3100

To determine whether hAECs home to the brain via CXCR4 signaling, mice were injected i.p. with either the specific C-X-C chemokine receptor type four (CXCR4) antagonist, AMD3100 (Sigma-Aldrich), or vehicle (0.9 % saline). AMD3100 (1 mg/kg) was administered 1 h prior to and 4 h after induction of 30 min MCAO. These mice received 1x10^6 CFSE-labeled hAECs i.v. at 1.5 h after induction of MCAO.

Functional assessment in the MCAO model of stroke

Mice subjected to filament-induced cerebral ischemia were assessed for functional deficits at either 30 min prior to euthanasia (i.e. at 23.5 h for the acute hAEC administration protocol) or on 0 d, 3 d, 7 d, 10 d and 14 d post-stroke (for the delayed hAEC administration protocol). This comprised a 5-point scoring system for neurological deficit: 0=normal motor function, 1=flexion of torso and contralateral forelimb when lifted by the tail, 2=circling to the contralateral side when held by the tail on a flat surface but normal posture at rest, 3=leaning to the contralateral side at rest, 4=no spontaneous motor activity. A hanging grip test was performed as a measure of grasping ability and forelimb grip strength[3, 6] in which mice were suspended by their forelimbs on a wire between two posts 60 cm above a soft pillow. The time until the animal fell was recorded (a score of 0 s was assigned to animals that fell immediately and a score of 60 or 120 s, where indicated, was assigned to animals that did not fall) and the average time of 3 trials with 5 min rests in between was calculated. An adhesive removal test was used to assess damage to the sensorimotor cortex of the mice; infarct damage typically involves this region in this model of stroke[20]. A small sticker was placed on each forepaw and the time taken to remove the stickers (up to a maximum of 180 s) was recorded and averaged from 3 trials, between which a resting period of 5 min was allowed.

Functional assessment in the photothrombotic model of stroke

Animals were tested once on each of the grid-walking and cylinder tasks one week prior to surgery to establish baseline performance levels. Animals were then tested at weeks 1, 2, 4, 6 and 8 post-stroke at approximately the same time each day (at the end of their dark cycle). Behaviors were scored by observers blinded to the treatment group, as described[7, 8].

MR imaging of cerebral infarcts

MR scans were performed at Monash Biomedical Imaging Facility using an echo planar capable, 9.4-T small animal MRI system (Agilent Technologies). Scans were performed in anesthetized (1 % isoflurane) mice at 1 d, 2 d and 3 d post-stroke, or marmosets at 1 d and 10 d post-stroke. The parameters of T2-weighted imaging acquisition in mice were: thickness=0.5 mm; repetition time=3500 ms; echo time=12.0 ms; echo train length=8; averages=6; flip angle=90°. Parameters of T2-weighted imaging acquisition in marmosets

were: 94 coronal slices with slice thickness=0.4 mm, no gap; repetition time=6,500 ms; echo time=39.1 ms; echo train length=4; flip angle=90°; field of view=38.4 x 38.4 mm^2, data matrix=192 x 192; 4 signal averages; scan time 21min.

Infarct analysis by thionin staining

Mice were euthanized by inhalation of isoflurane and the brain was either immediately removed, frozen in liquid nitrogen, and stored at -80 ° C (MCAO model) or perfuse-fixed with 4 % paraformaldehyde and preserved in sucrose (photothrombotic model). For the MCAO model, evenly spread (separated by ~420 μm) coronal sections (30 μm thick) were obtained spanning the infarct, and thaw-mounted onto poly-L-lysine coated glass slides. For the photothrombotic model, evenly spread (separated by ~210 μm) coronal sections (30 μm thick) were obtained spanning the infarct and mounted on gelatin-coated slides. Sections were stained with thionin (0.1 %) to delineate the infarct, and infarct volume was calculated as described[3, 21].

Locating hAECs in the brain and spleen

Frozen brains and spleens were sectioned (10 μm) and thaw-mounted onto poly-L-lysine coated glass slides. Serial coronal sections spanning the infarct (bregma +0.84 mm, +0.42 mm, 0 mm, -0.42 mm. -0.84 mm, -1.26 mm, -1.68 mm and -2.10 mm) and six sections per spleen were taken for analysis. After cutting, the sections were immediately analyzed for CFSE: images were captured using an Olympus fluorescent microscope (BX51, Japan) and analyzed by two observers blinded to the identity of the treatment.

Immunohistochemistry

Immunohistochemistry was performed as described previously[4, 22]. Sections were fixed with either ice-cold acetone or 4 % paraformaldehyde (if not previously perfused-fixed), washed in 0.01 M phosphate-buffered saline, and incubated in 10 % goat-serum for 1 h to block non-specific staining. For diaminobenzidine (DAB, Dako) staining, endogenous peroxidases were also blocked with peroxidase blocking solution (Dako). All sections were incubated with primary antibodies (Table I) overnight at either room temperature or 4 °C. The following day, tissues were washed, and then incubated for a maximum of 2 h with the relevant secondary antibody (Table I). For DAB staining, sections were then washed and DAB was applied for 5-10 min. For immunofluorescence staining, sections were counterstained with 4',6-diamidino-2-phenylindole (DAPI). Finally, all sections were washed, dehydrated in ascending concentrations of ethanol if required (Table I), mounted with appropriate mounting medium (Table I) and a coverslip applied. When using a primary antibody that was raised in a mouse, we used the Mouse-on-Mouse kit (Vector Laboratories) as per supplied protocol. Tissue-mounted slides were viewed and photographed with either an Olympus fluorescence/light microscope or NikonA1 inverted confocal microscope. Analysis of stained sections was performed in a blinded manner wherever possible and all appropriate controls were performed to ensure antibody specificity.

Image processing and quantification of MAP2, GFAP and GAD67 staining

For MAP2/GFAP double-labeled sections and GAD67 single-labeled sections, images were taken on a NikonA1 inverted confocal at 10x magnification and processed in FIJI image analysis software (NIH). Regions of interests (ROI) were defined and saved using the ROI Manager. For each image the selections used for the ROI were copied across and moved into the correct area in order to standardize between section analysis. The integrated density value (IDV) was measured in all ROI across the three channels using the Multi Measure tool in ROI Manager. To calculate the average cell number for each ROI the three channels were

split. Using the blue channel, a selection of at least 10 representative nuclei in the ROI were outlined and measured for integrated density. Dividing the blue channel IDV of each ROI by the mean nucleus IDV gives the average number of cells present in each ROI. The fluorescent intensity for both the green and orange channels was expressed as a per-cell measure by dividing the IDV for each ROI by its respective average cell number. For cell counts, MAP2 and GFAP expression, IVDs were normalised to sham control levels. For GAD67, the whole image was selected as the ROI and the mean fluorescent intensity was measured through a single channel.

Flow cytometry

Mice were euthanized and brain (ischemic hemisphere), blood, spleen, lymph nodes and bone marrow were harvested. Single cell suspensions were prepared as described[23-25]. Cells were stained with Live/Dead cell stains and appropriate antibodies (listed below), and run on either an LSRII (BD Biosciences) or Gallios (Beckman Coulter) instrument. Single-stain spleen samples or bead controls (OneComp or UltraComp ebeads, eBiosciences) were used to adjust voltages and calculate compensation for each corresponding antibody. Fluorescence minus one controls were used where the antibody of interest was omitted. Data were analyzed using either FlowJo (Tree Star Inc) or Kaluza (Beckmann Coulter) software. Three panels of antibodies were used for flow cytometry experiments. For leukocyte quantification within brains, the following cocktail of antibodies was used: anti–CD45–APC-Cy7 (30-F11), anti-CD11b-Pacific Blue (M1/70), anti-Ly6G-PE-Cy7 (1A8) (all from Biolegend), anti-CD8a-APC (53-6.7) (BD Biosciences), anti-CD4-Pacific Orange (RM4-5) (Life Technologies) and anti-B220-PE (RA3-6B2) (eBioscience). For leukocyte quantification of blood and spleen in young male mice, we used the following cocktail of antibodies: anti-CD45-APC-Cy7 (30-F11), anti-Ly6C-FITC (HK1.4), anti-Ly6G-PE-Cy7 (1A8), anti-CD8a-BV785 (53-6.7) (all from BioLegend), anti-CD11b-Pacific Blue (M1/70), anti-CD19-PE (MB19-1), anti-CD3e-APC (145-2011) and anti-CD4-AF 700 (GK1.5) (all from eBiosciences). For leukocyte quantification in blood, spleen, lymph nodes and bone marrow of aged female mice we the following antibodies: anti-CD11b-APC (M1/70), anti B220-FITC (RA3-6B2), (both from BioLegend) and anti-CD3e-PE-CF594 (145-2C11) (BD Biosciences). Dead cells were labeled with 7-aminoactinomycin D (7AAD; Life Technologies), LIVE/DEAD® fixable aqua dead cell stain (Life Technologies) or LIVE/DEAD® fixable violet dead cell stain (Life Technologies).

Primary cortical neuronal cultures and glucose deprivation

Primary neuronal cultures were prepared from cerebral cortices of embryonic day (E)17 C57Bl6 mouse embryos as described[26]. Briefly, cortices were dissected, and digested in trypsin (1 mg/ml; Sigma) for 10 min followed by neutralization with trypsin inhibitor (1.5 mg/ml; Sigma). Dissociated cells were resuspended in Neurobasal medium (Gibco) supplemented with B27® (2 %; Gibco), HEPES (20 mM), GlutaMax (1.3 mM; Gibco) and gentamicin (25 μg/ml; Gibco), then plated onto poly-D-lysine coated 60 mm^2 Petri dishes. Cells were then incubated overnight in a humidified incubator. The following day, media was replaced with fresh Neurobasal media containing supplements, and cells were maintained for a further 8 d with renewal of half medium every 3-4 d. For glucose deprivation experiments, cultured primary neurons (9 d in vitro) were incubated in glucose-free Locke's buffer as described[26]. Neurons received one of the following treatments: (i) control (no treatment); (ii) vehicle (Locke's buffer only); (iii) hAECs (10^4 or 10^5 per dish at the commencement of glucose deprivation). Cell viability was determined 24 h later using trypan blue exclusion. Approximately 300 cells were counted manually from each dish with the assistance of image analysis software (ImageJ, NIH).

Western blot

Western blots were performed as previously described[27]. Brain protein samples were subjected to sodium dodecyl sulfate–polyacrylamide (10 %) gel electrophoresis using a Tris-glycine running buffer. Gels were then electro-blotted using a transfer apparatus (Bio-Rad Laboratories, Inc.) in transfer buffer containing 0.025 mol/l Tris base, 0.15 mol/l glycine, and 10 % (v/v) methanol for 1.5 h at 15 V onto a nitrocellulose membrane (Bio-Rad Laboratories, Inc.). The membrane was then incubated in blocking buffer (5 % skim milk in 20 mM Tris-HCl, pH 7.5, 137 mM NaCl, 0.2% Tween-20) for 1 h at 23 °C. The membrane was then incubated overnight at 4 °C with primary antibodies including, cleaved caspase-3 (Cell Signaling), caspase-8, cleaved-caspase-8 and NLRP3 (all from Adipogen), and *β*-actin (Sigma-Aldrich). After washing (3x10 min) with Tris-buffered saline-T (20 mM Tris-HCl, pH 7.5, 137 mM NaCl, 0.2 % Tween-20), the membrane was incubated with secondary antibodies against the primary antibody and *β*-actin for 1 h at room temperature. The membrane was washed with Tris-Buffered saline-T and scanned using the Odyssey Infrared Imaging System (LI-COR Biosciences). Quantification of protein was achieved by densitometry analysis using Image J software.

Quantitative real-time PCR

Total RNA was isolated from spleens of male mice 72 h post-MCAO or sham surgery using TRIzol® reagent (Thermofisher Scientific) and the RNeasy Mini Kit with on-column DNase step (Qiagen) followed by cDNA conversion using the Quantitect Reverse Transcription kit (for Taqman® gene expression assays; Qiagen). Pre-designed Taqman® gene expression assays were then used to measure mRNA expression of *Tbx21*, *Stat4*, *Gata3*, *Stat6*, *Foxp3*, *Rorc* and *β-actin* as a house-keeping gene. Assays were performed according to the manufacturer's instructions using the Bio-Rad CFX96TM real-time PCR machine (Bio-Rad). Data were normalized to the housekeeping gene and calculated as changes in fold-expression relative to sham using the formula: fold-change = $2^{-\Delta\Delta CT}$.

Bacterial analysis in lungs

Mice were euthanized by inhaled isoflurane overdose and the skin washed with 70 % ethanol under sterile conditions. Lungs were removed and homogenized in sterile PBS. To determine colony forming units (CFU), 10 µL of tissue homogenate was serially diluted, plated onto brain heart infusion agar plates supplemented with 5 % sheep blood, incubated at 37 °C for 18 h, and bacterial colonies were counted.

Mouse embryonic stem cells (ESCs)

Briefly, E14Tg2a mouse ESCs (ATCC) were maintained in mESC medium of DMEM containing GlutaMAX™-I supplemented with 10 % FBS (ES qualified), 100 units/ml penicillin/streptomycin, 0.1 mM β-mercaptoethanol (all from Gibco) and 10^3 units/ml Leukemia Inhibitory Factor (Merck Millipore). Cells were passaged on 0.1 % gelatin-coated culture plates every other day. For neural differentiation, cells were seeded at 5 x 10^3 cells/cm^2 and 48 h later they were induced with a 1:1 mixture of Neurobasal® and DMEM/F-12 supplemented with N2 and B27®, 0.005 % Fraction V Bovine Serum Albumin (all from Gibco) and 1 mg/ml Bovine insulin (Gemini Bio-products). Two to four days later cells were dissociated (Accutase®, Innovative Cell Technologies) and resuspended in saline in preparation for transplantation.

Statistical analysis

Data are typically presented as a combined scatter plot with mean ± standard error, with the exception of neurological deficit scores, which are presented as scatter plot with median. Statistical analyzes were performed using GraphPad Prism version 6.0 (GraphPad Software Inc., San Diego, CA, USA). Outliers were identified by a ROUT test using GraphPad Prism and excluded where appropriate. Between-group comparisons were compared using one-way ANOVA, or two-tailed Student's unpaired t-test, where appropriate. If differences were detected by ANOVA, individual groups were compared with the Newman-Keuls or Tukey's multiple comparison test, where indicated. Neurological deficit scores were compared using a Mann-Whitney test or if there were more than two groups, a Kruskal-Wallis test followed by Dunn's multiple comparisons test. Survival data was analyzed using a log-rank test. If there were two independent variables, data were compared using a two-way ANOVA, followed by either Bonferroni's or Tukey's multiple comparison test, where indicated. Statistical significance was accepted as $P<0.05$.

Table I. Antibody concentrations, incubation temperatures and mounting conditions for immunohistochemistry experiments.

Primary antibody	Dilution	Incubation temperature	Secondary antibody	Dilution	Mounting media
Rabbit anti-cleaved caspase-3 (Abcam; ab2302)	1:200	Room temperature	Goat-anti-rabbit IgG Alexa Fluor 594 (Life Technologies)	1:500	Vectashield (Vector Laboratories)
Rabbit anti-annexin V (Abcam; ab14196)	1:200	Room temperature	Goat-anti-rabbit IgG Alexa Fluor 594 (Thermofisher)	1:500	Vectashield (Vector Laboratories)
Mouse anti-NeuN (Chemicon; MAB377)	1:1000	Room temperature	MOM™ biotinylated anti-mouse IgG reagent (Vector Laboratories)	1:200	Vectashield (Vector Laboratories)
Rabbit-anti-CD3 (Abcam; Ab16669)	1:200	Room temperature	Goat-anti-rabbit IgG Alexa Fluor 594 (Thermofisher)	1:500	Vectashield (Vector Laboratories)
Rat anti-F4/80 (BioRad; MCA497G)	1:100	Room temperature	Goat-anti-rabbit IgG Alexa Fluor 594 (Thermofisher)	1:500	Vectashield (Vector Laboratories)
Mouse anti-3-nitrotyrosine (Abcam; ab61392)	1:50	Room temperature	MOM™ biotinylated anti-mouse IgG reagent (Vector Laboratories)	1:200	Vectashield (Vector Laboratories)
Rabbit anti-GFAP (Abcam; ab7260)	1:500	Room temperature	Goat-anti-rabbit IgG Alexa Fluor 488 (Thermofisher)	1:500	Vectashield (Vector Laboratories)
Rabbit-anti-myeloperoxidase (Abcam; ab9535)	1:100	Room temperature	Anti-rabbit IgG horse-radish peroxidase conjugate (Dako)	1:200	DPX (after ethanol dehydration and xylene clearing)
Rabbit anti-MAP2 (Millipore; AB5622)	1:500	4°C	Donkey anti-rabbit IgG DyLight 488 (Thermofisher)	1:800	DPX (after ethanol dehydration and xylene clearing)
Chicken anti-GFAP (Millipore; AB5541)	1:3000	4°C	Donkey anti-chicken IgY AlexaFluor 568 (Thermofisher)	1:800	DPX (after ethanol dehydration and xylene clearing)
Mouse anti-GAD67 (Chemicon; MAB5406)	1:500	4°C	Donkey anti-mouse Dylight 488 (Thermofisher)	1:800	DPX (after ethanol dehydration and xylene clearing)

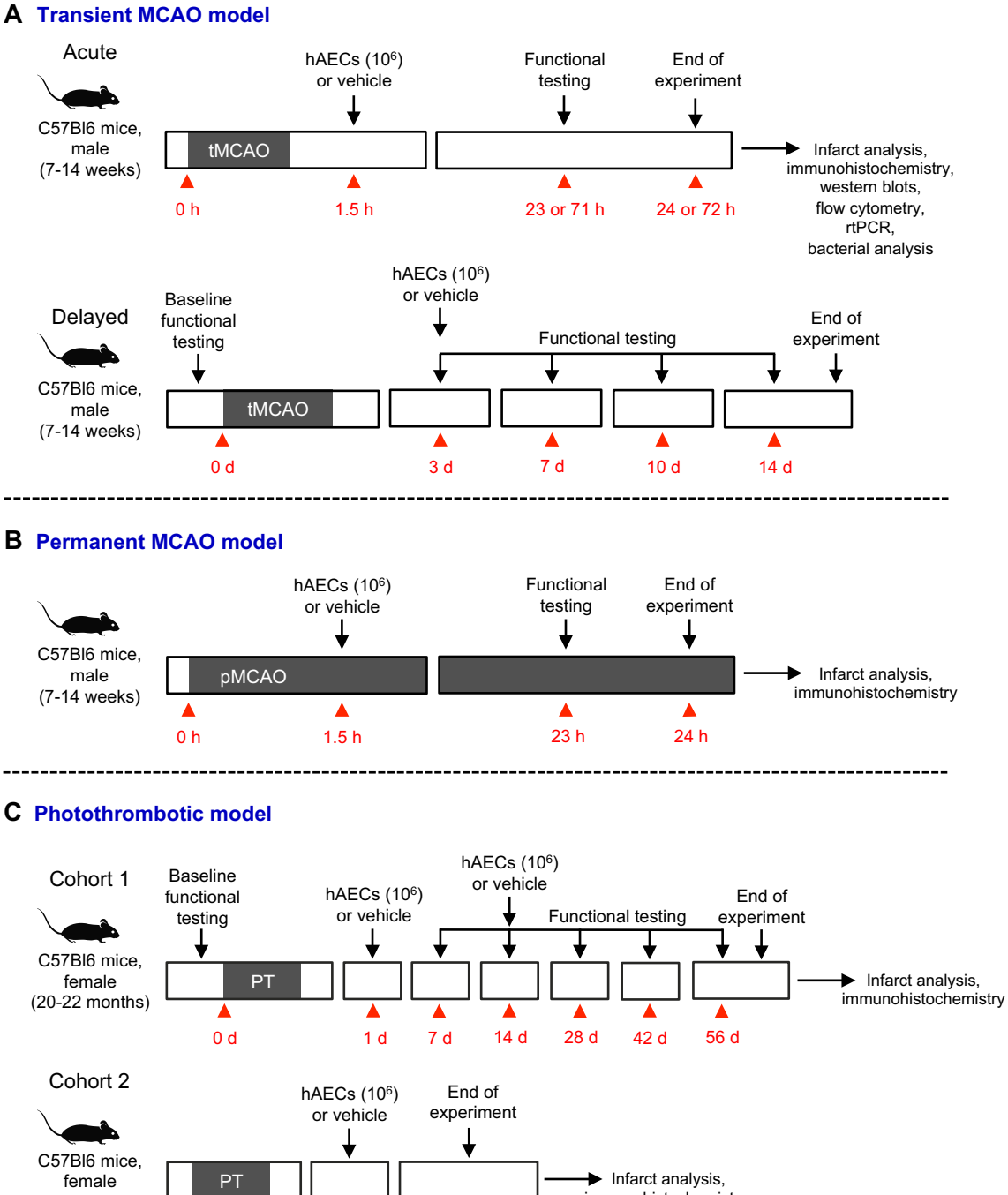
A Transient MCAO model
Acute
C57Bl6 mice, male (7-14 weeks)
hAECs (10⁶) or vehicle
Functional testing
End of experiment
tMCAO
0 h
1.5 h
23 or 71 h
24 or 72 h
Infarct analysis, immunohistochemistry, western blots, flow cytometry, rtPCR, bacterial analysis
Delayed
C57Bl6 mice, male (7-14 weeks)
Baseline functional testing
hAECs (10⁶) or vehicle
Functional testing
End of experiment
tMCAO
0 d
3 d
7 d
10 d
14 d
B Permanent MCAO model
C57Bl6 mice, male (7-14 weeks)
hAECs (10⁶) or vehicle
Functional testing
End of experiment
pMCAO
0 h
1.5 h
23 h
24 h
Infarct analysis, immunohistochemistry
C Photothrombotic model
Cohort 1
C57Bl6 mice, female (20-22 months)
Baseline functional testing
hAECs (10⁶) or vehicle
hAECs (10⁶) or vehicle
Functional testing
End of experiment
PT
0 d
1 d
7 d
14 d
28 d
42 d
56 d
Infarct analysis, immunohistochemistry
Cohort 2
C57Bl6 mice, female (20-22 months)
hAECs (10⁶) or vehicle
End of experiment
PT
0 d
1 d
7 d
Infarct analysis, immunohistochemistry, flow cytometry
D Endothelin-1 model
Marmosets, male and female (3-5 years)
hAECs (10⁶) or vehicle
MRI
MRI
End of experiment
ET-1
0 h
1.5 h
1 d
10 d

Figure I. Timeline showing the animal models of stroke used in this study. **A,** Young male mice (7-14 weeks) were subjected to transient middle cerebral artery occlusion (tMCAO) and received either vehicle or hAECs (10^6) at either 1.5 h (acute) or 3 d (delayed) post-stroke. Functional outcome was assessed at the timepoints indicated, and at the end of the experiment organs were harvested for analysis. **B,** Young male mice (7-14 weeks) were subjected to permanent middle cerebral artery occlusion (pMCAO) and received either vehicle or hAECs (10^6) at 1.5 h post-stroke. Functional outcome was assessed at approximately 23 h post-stroke, and at the end of the experiment brains were harvested for analysis. **C,** Cohort 1: Aged female mice (20-22 months) were subjected to photothrombotic stroke (PT) of the primary motor cortex and received either vehicle or hAECs (10^6) at 1±14 d post-stroke. Functional outcome was assessed over 56 d, and at the end of the experiment brains were removed for analysis. Cohort 2: Aged female mice were subjected to photothrombotic stroke and received either vehicle or hAECs (10^6) at 1 d post-stroke. At the end of the experiment, brains and lymphoid organs were removed for analysis. **D,** Adult marmosets (3-5 years; male and female) were subjected to endothelin-1 (ET-1) -induced ischemia of the primary visual cortex and received either vehicle or hAECs ($5x10^6$) at 1.5 h post-stroke. Magnetic resonance imaging was performed to measure infarct volume at 1 d and 10 d post-stroke.

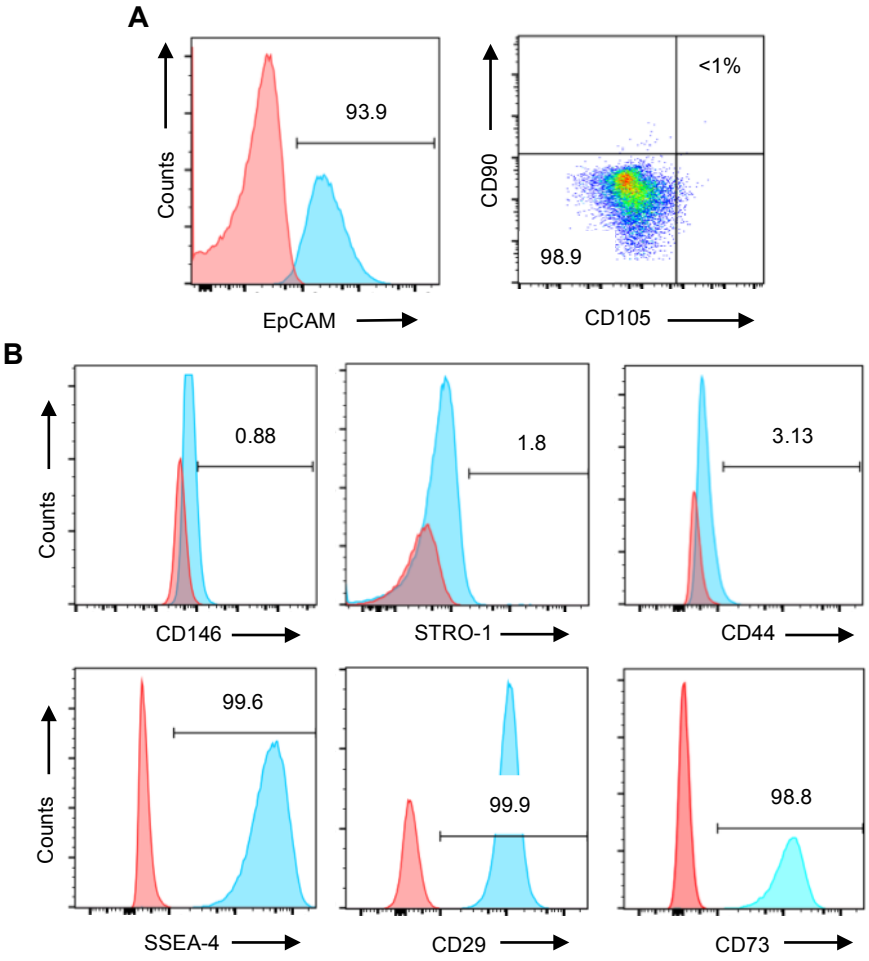

Figure II. Characterization of human amnion epithelial cells (hAECs). **A,** Primary hAEC isolates were gated positive for epithelial cell marker EpCAM and negative for mesenchymal stromal markers CD90 and CD105. **B,** Cells that were $EpCAM^{+}CD90^{-}CD105^{-}$ were further gated for the stem cell and stromal markers CD146, STRO-1, CD44, SSEA-4, CD29 and CD73.

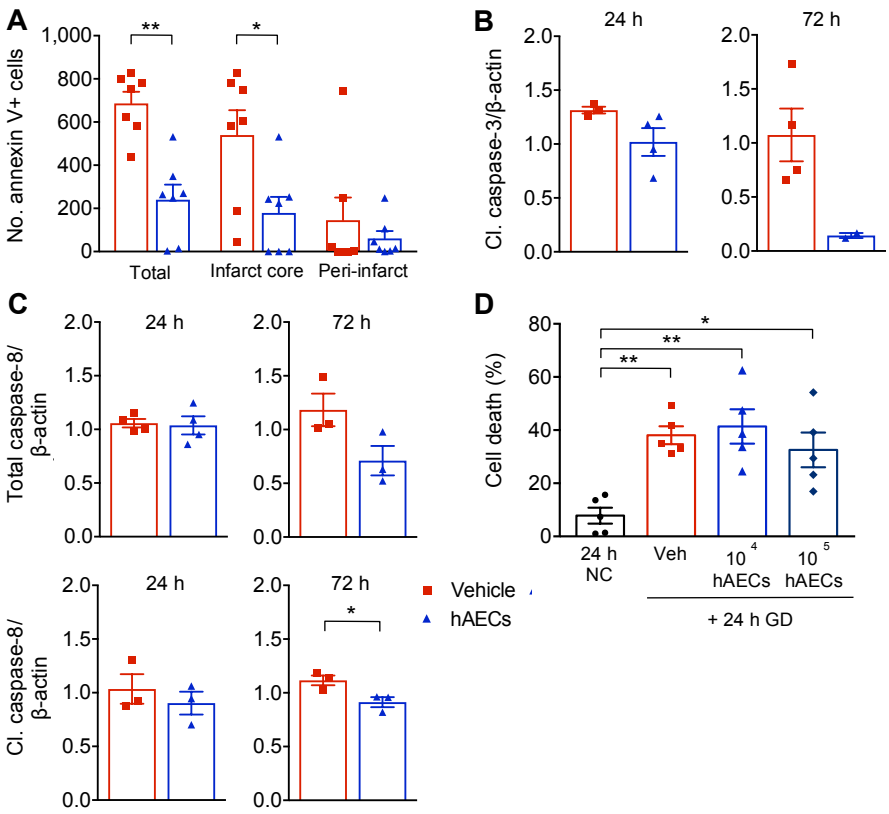

Figure III. Human amnion epithelial cells (hAECs) reduce cerebral apoptosis *in vivo* but provide limited direct protection against neuronal cell death *in vitro*. *In vivo*: Young male mice were subjected to 30 min MCAO and were injected with either vehicle or hAECs 1.5 h post-stroke. **A**, Immunohistochemistry was used to quantify annexin V-positive cells within the infarct core and peri-infarct region at 72 h post-stroke (n=7 per group). Western blotting was used to quantify whole brain protein expression of: **B**, cleaved-caspase 3 (n=2-4 per group) as well as **C**, total and cleaved caspase-8 (n=3-4 per group). *In vitro:* primary neuronal cultures were exposed to either normal conditions (NC) or glucose deprivation (GD) for 24 h. **D**, Glucose-deprived cultures were treated with either vehicle or hAECs (10^4 or 10^5 cells per dish) and dead cells were quantified (n=5 per group). *P<0.05, **P<0.01, two-way ANOVA (A), Student's unpaired t-test (C) or one-way ANOVA followed by Tukey's multiple comparison test (D). Data are presented as mean ± SEM.

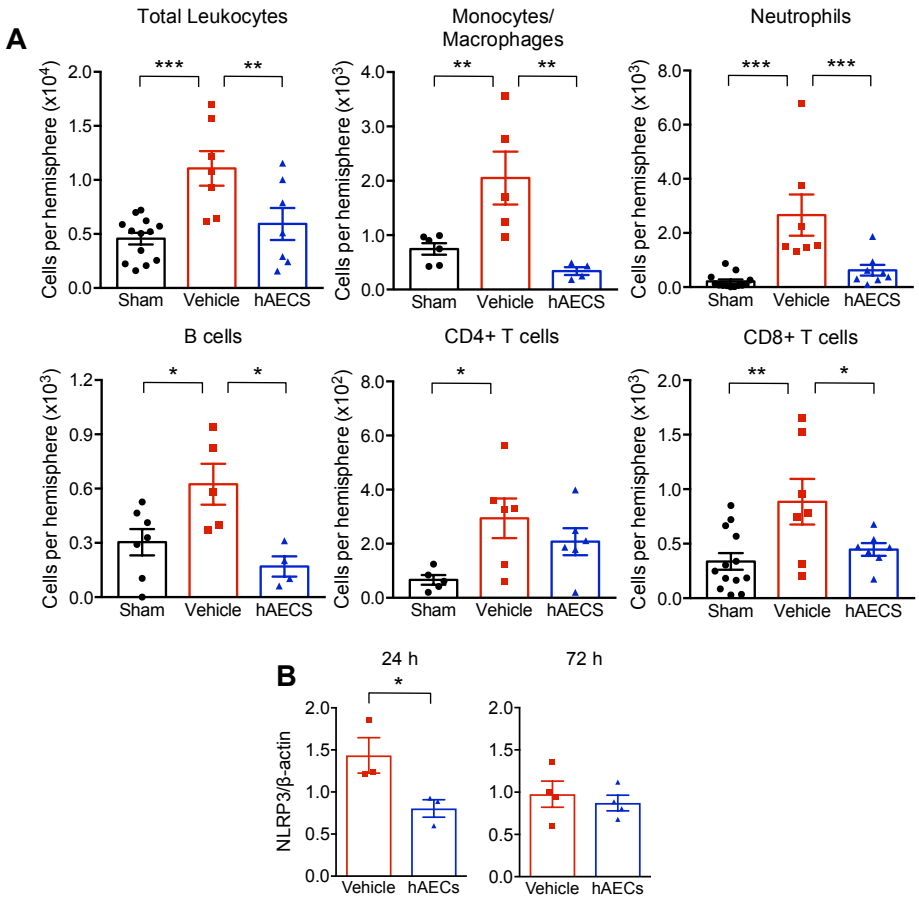

Figure IV. Human amnion epithelial cells (hAECs) reduce post-stroke inflammation. Young male mice were subjected to either sham surgery or 30 min MCAO and were injected with either vehicle or hAECs 1.5 h later. **A**, Flow cytometry was performed to quantify: total leukocytes, monocytes/macrophages, neutrophils, B cells, CD4+ T cells and CD8+ T cells in the right/ischemic brain hemisphere of sham, vehicle- and hAECs-treated mice at 24 h post-surgery (n=4-13 per group). **B,** Western blot analysis of nod-like receptor protein 3 (NLRP3) expression in the brain of hAECs- and vehicle- treated mice at 24 and 72 h post-stroke (n=3-4 per group). *P<0.05, **P<0.01, ***P<0.001, one-way ANOVA, followed by Newman-Keuls multiple comparison test (A) or Student's unpaired t-test (B). Data are presented as mean ± SEM.

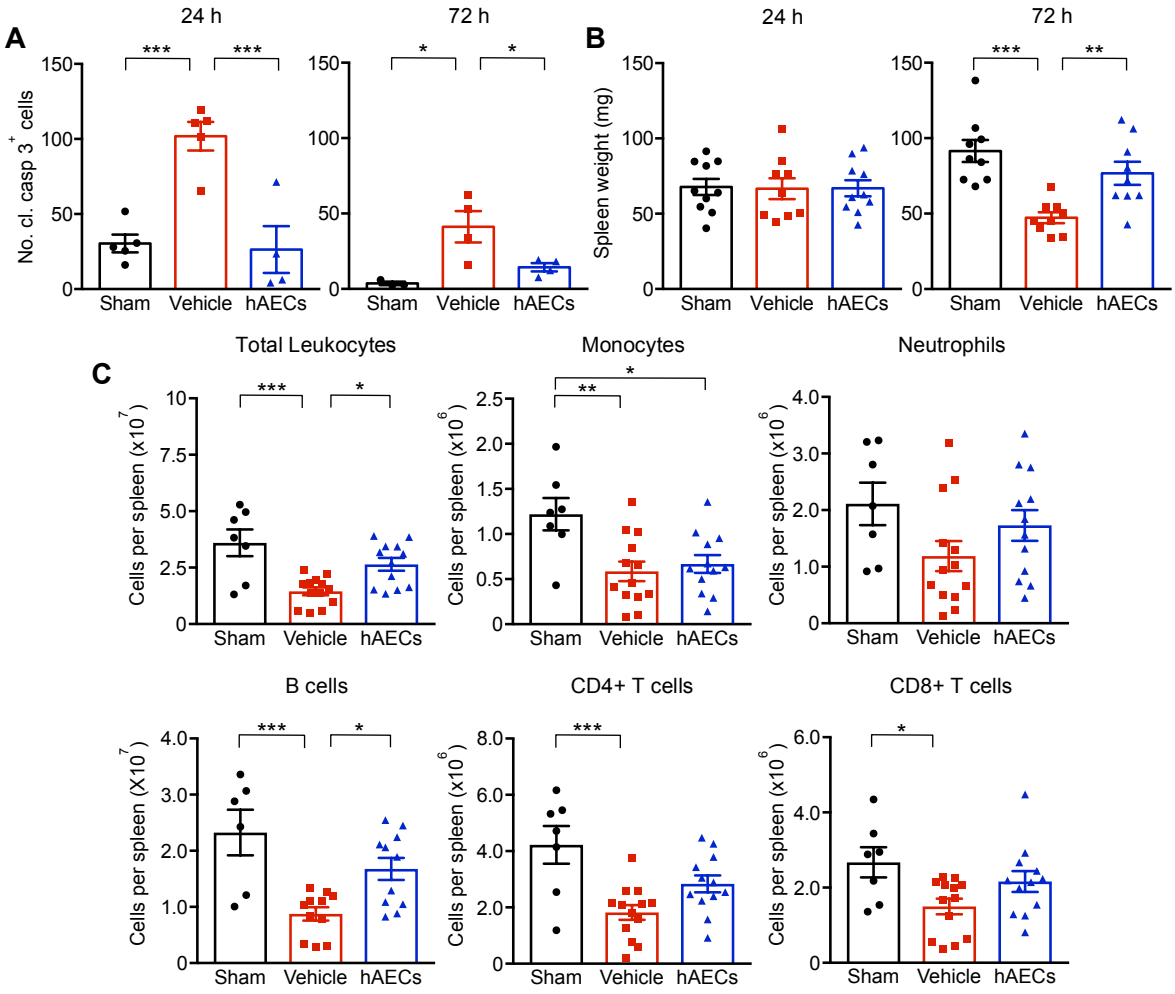

Figure V. Acute administration of hAECs blunts hallmarks of stroke-induced systemic immunosuppression. Young male mice were subjected to either sham surgery or 60 min MCAO and were injected with either vehicle or hAECs 1.5 h later. At 24 or 72 h post-surgery spleens were removed for analysis. **A**, Number of immunoreactive cleaved-caspase 3+ (cl. casp 3+) splenocytes at 24 and 72 h post-stroke (n=3-5). **B**, Spleen weights at 24 and 72 h post-stroke (n=9-10). **C**, Flow cytometric analysis of splenic: total leukocytes, monocytes, neutrophils, B cells, CD4+ T cells and CD8+ T cells at 72 h post-stroke (n=6-13). *P<0.05, **P<0.01, ***P<0.001, one-way ANOVA followed by Tukey's multiple comparison test. Data are presented as mean±SEM.

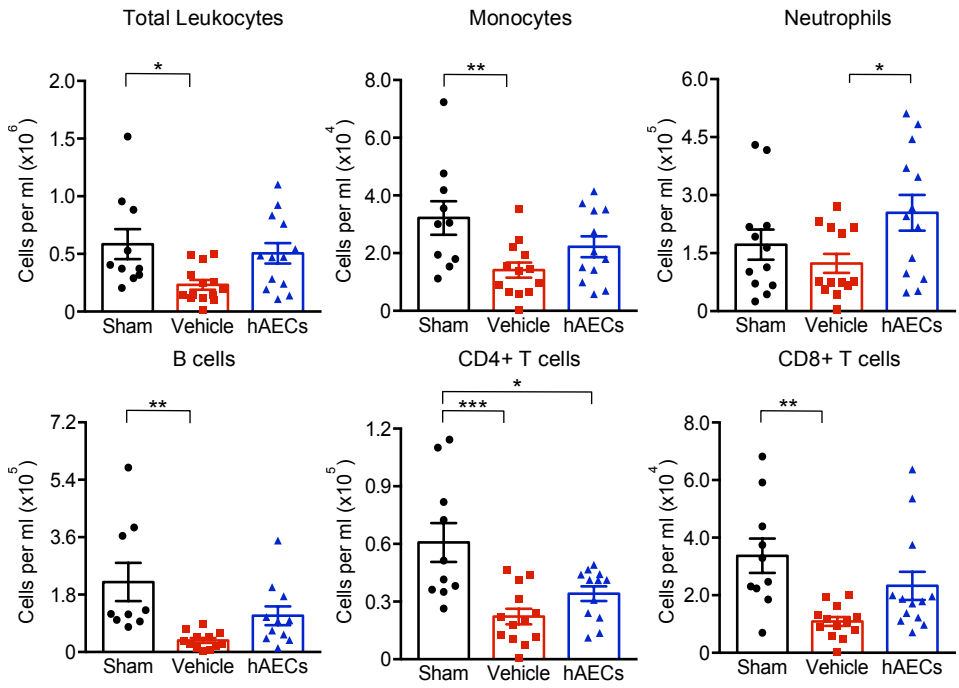

Figure VI. Young male mice were subjected to either sham surgery or 60 min MCAO and were injected with either vehicle or hAECs 1.5 h later. At 72 h post-surgery blood was withdrawn for analysis by flow cytometry. Numbers of circulating: total leukocytes, monocytes, neutrophils, B cells, CD4+ T cells and CD8+ T cells (n=9-13). *P<0.05, **P<0.01, ***P<0.001, one-way ANOVA followed by Tukey's multiple comparison test. Data are presented as mean±SEM.

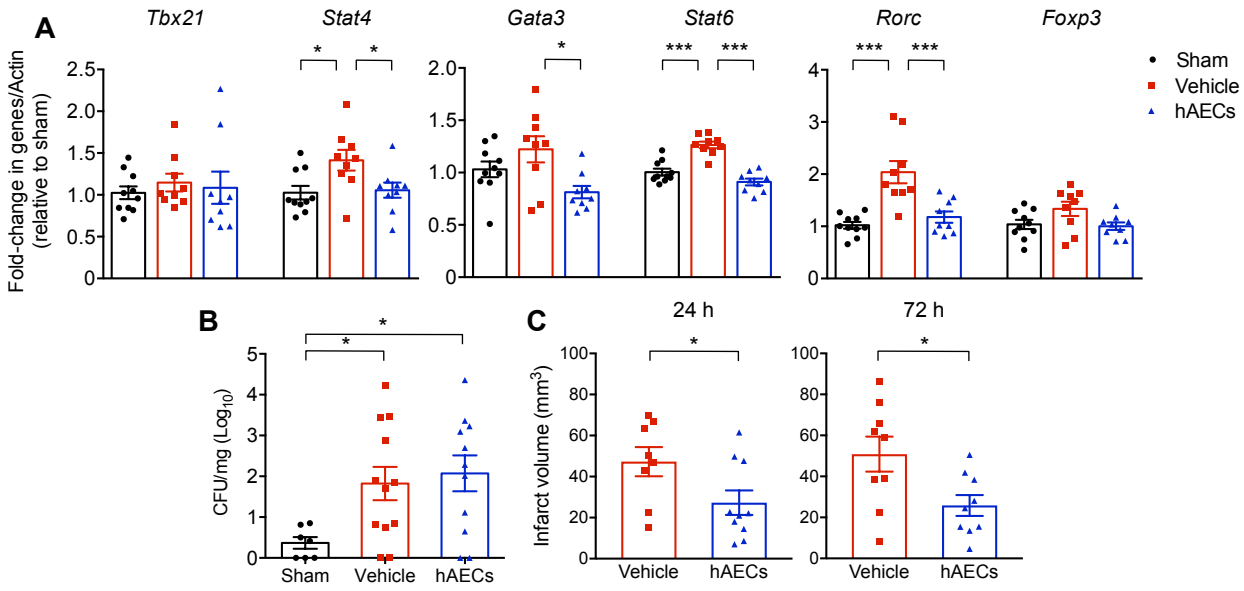

Figure VII. Human amnion epithelial cells (hAECs) reduce infarct volume and the expression of splenic T cell transcription factors but have no effect on post-stroke lung infections following stroke. Young male mice were subjected to either sham surgery or 60 min MCAO and were injected with either vehicle or hAECs 1.5 h later. **A,** mRNA expression of Th1 transcription factors *Tbx21* and *Stat4*, Th2 transcription factors *Gata3* and *Stat6*, Th17 transcription factor *Rorc* and T regulatory cell transcription factor *Foxp3* within the spleen of sham, vehicle- and hAECs-treated mice at 72 h post-surgery (n=9-10) per group. **B**, Lungs were collected for bacteriological analysis at 72 h post-surgery. Data are expressed as colony forming units (CFU)/mg lung tissue (Log_{10}) (n=7-12 per group). **C,** Infarct volume measured at 24 and 72 h following 60 min MCAO (n=8-10 per group). *P<0.05, ***P<0.001, one-way ANOVA, followed by Tukey's multiple comparison test (A), Newman Keuls multiple comparison test (B) or Student's unpaired t-test (C). Data are presented as mean ± SEM.

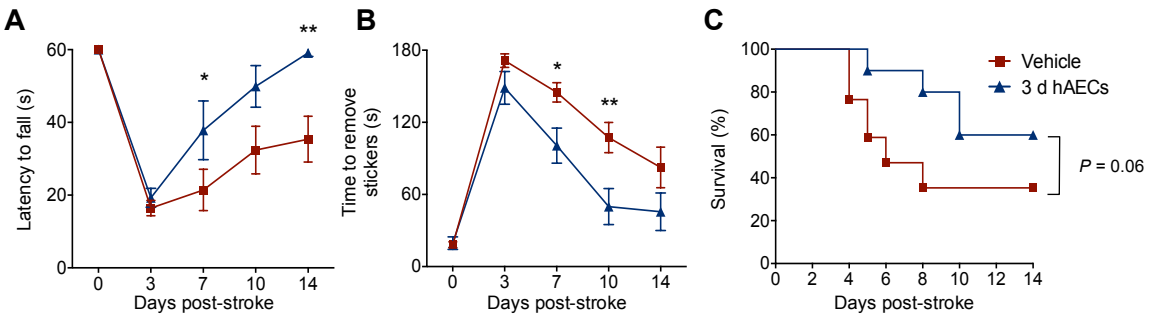

Figure VIII. Delayed administration of human amnion epithelial cells (hAECs) improves functional recovery following stroke. Young male mice were administered either hAECs or vehicle at 3 d post-30 min MCAO and functional recovery was assessed over 14 d. **A**, latency to fall in hanging grip test, **B,** latency to remove stickers on forepaws and **C,** survival of hAECs- and vehicle-treated mice over 3 to 14 d post-stroke (n=6-17). *P<0.05, **P<0.01, two-way ANOVA followed by Bonferroni's test or Log-rank test (for survival).

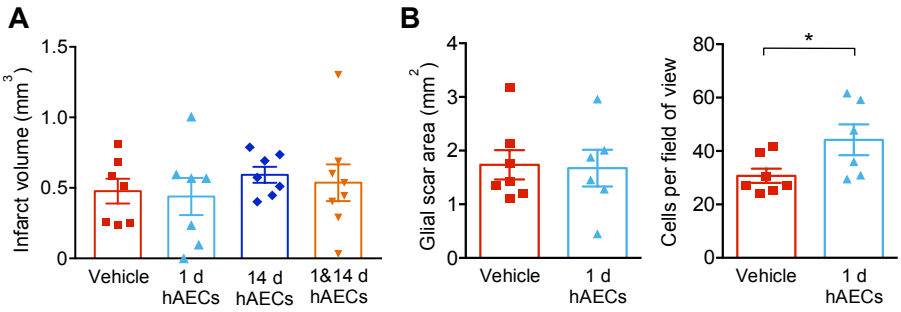

Figure IX. Human amnion epithelial cells (hAECs) do not alter infarct size in aged female mice at 56 d post photothrombtoic stroke, but increase glial scar density. **A**, Lesion volume at 56 d post-stroke (*n*=7-8 per group). **B**, Glial scar area and density at 56 d in mice treated with either hAECs or vehicle at 1 d post-stroke (*n*=6-7 per group). **P*<0.05, one-way ANOVA (A) or Student's unpaired t-test (B). Data are presented as mean ± SEM.

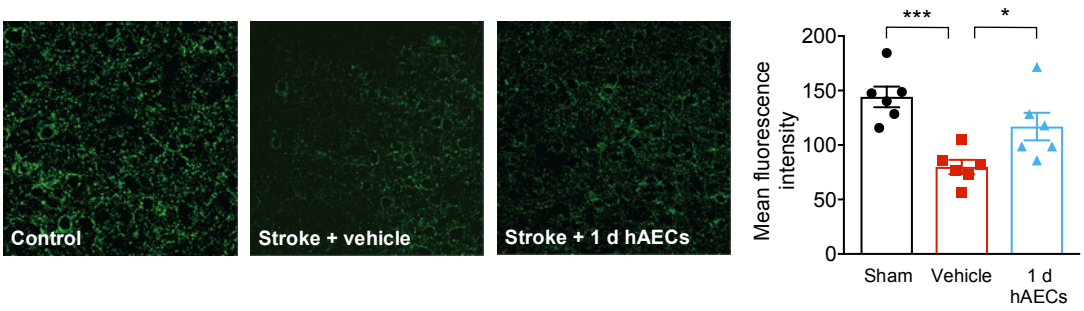

Figure X. Human amnion epithelial cells (hAECs) prevent the decrease in inhibitory interneurons within the peri-infarct cortex of aged-female mice following photothrombotic stroke. Immunofluorescence was performed to quantify the amount of glutamic acid decarboxylase-67 (GAD67) staining in the peri-infarct cortex in the brains of sham-, stroke + vehicle- and stroke + 1 d hAEC-treated animals at 7 d post-surgery (n=6 per group; data are expressed as mean fluorescence intensity). *P<0.05, ***P<0.001 (one-way ANOVA followed by Tukey's multiple comparison test). Data are presented as mean ± SEM

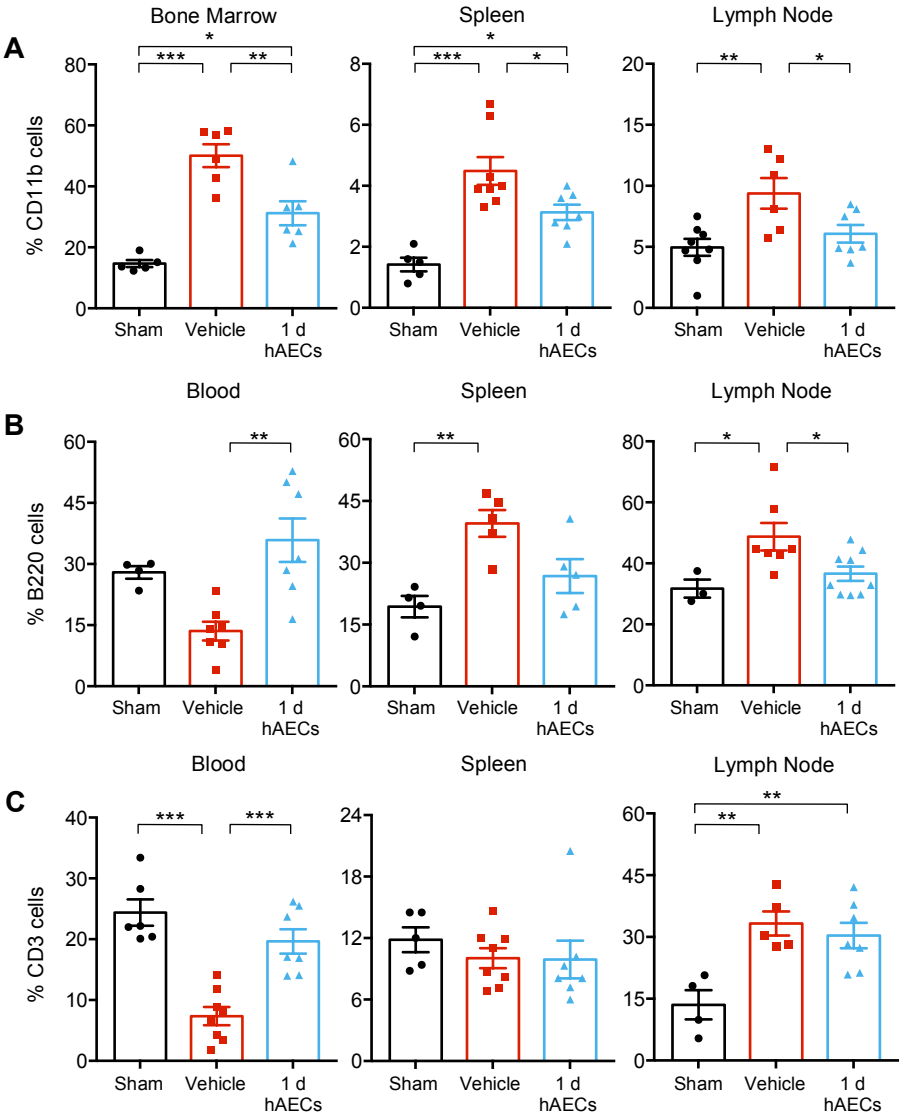

Figure XI. Human amnion epithelial cells (hAECs) modulate the systemic immune response to photothrombotic stroke in aged female mice. Flow cytometry was used to quantify the percentage of: **A**, myeloid CD11b+ cells (n= 5-8 per group), **B**, B220+ B cells (n=3-9 per group) and **C,** CD3+ T cells (n=4-8 per group) within the blood or bone marrow, spleen and lymph node at 7 d after stroke. *P<0.05, **P<0.01, ***P<0.001, one-way ANOVA followed by Tukey's multiple comparison test. Data are presented as mean ± SEM.

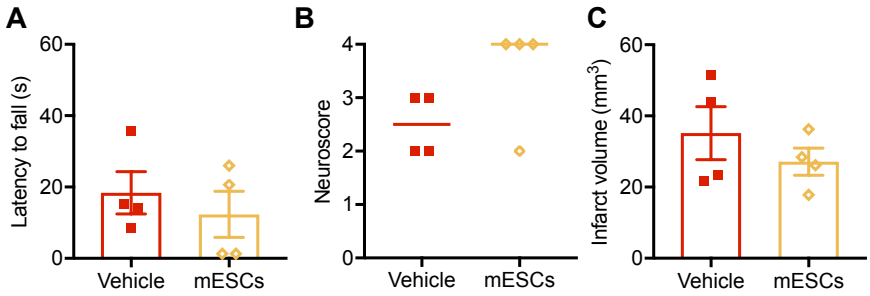

Figure XII. Administration of mouse embryonic stem cells (mESCs) has no effect on post-stroke outcomes. Young male mice were subjected to either sham surgery or 30 min MCAO and were injected with either vehicle or mESCs. Functional outcome and/or infarct volume was assessed at 24 post-stroke. **A,** Latency to fall on hanging grip test (*n*=4 per group). **B,** Median neurological deficit score (*n*=4 per group). **C,** Infarct volumes measured using thionin staining (*n*=4 per group). Data are presented as ± SEM.

References

1. Recommendations for standards regarding preclinical neuroprotective and restorative drug development. *Stroke*. 1999;30:2752-2758
2. Savitz SI, Chopp M, Deans R, Carmichael T, Phinney D, Wechsler L, et al. Stem cell therapy as an emerging paradigm for stroke (steps) ii. *Stroke*. 2011;42:825-829
3. Brait VH, Jackman KA, Walduck AK, Selemidis S, Diep H, Mast AE, et al. Mechanisms contributing to cerebral infarct size after stroke: Gender, reperfusion, t lymphocytes, and nox2-derived superoxide. *J. Cereb. Blood Flow Metab.* 2010;30:1306-1317
4. Broughton BR, Brait VH, Kim HA, Lee S, Chu HX, Gardiner-Mann CV, et al. Sex-dependent effects of g protein-coupled estrogen receptor activity on outcome after ischemic stroke. *Stroke*. 2014;45:835-841
5. López-Valdés HE, Clarkson AN, Ao Y, Charles AC, Carmichael ST, Sofroniew MV, et al. Memantine enhances recovery from stroke. *Stroke*. 2014;45:2093-2100
6. Broughton BR, Brait VH, Guida E, Lee S, Arumugam TV, Gardiner-Mann CV, et al. Stroke increases g protein-coupled estrogen receptor expression in the brain of male but not female mice. *Neurosignals*. 2012
7. Clarkson AN, Huang BS, Macisaac SE, Mody I, Carmichael ST. Reducing excessive gaba-mediated tonic inhibition promotes functional recovery after stroke. *Nature*. 2010;468:305-309
8. Clarkson AN, Parker K, Nilsson M, Walker FR, Gowing EK. Combined ampakine and bdnf treatments enhance poststroke functional recovery in aged mice via akt-creb signaling. *J Cereb Blood Flow Metab*. 2015;35:1272-1279
9. Teo L, Bourne JA. A reproducible and translatable model of focal ischemia in the visual cortex of infant and adult marmoset monkeys. *Brain Pathol.* 2014;24:459-474
10. Lapchak PA, Zhang JH, Noble-Haeusslein LJ. Rigor guidelines: Escalating stair and steps for effective translational research. *Transl Stroke Res*. 2013;4:279-285
11. Yano C, Iwata M, Uchiyama S. Risk factors for small cortical infarction on diffusion-weighted magnetic resonance imaging in patients with acute ischemic stroke. *J. Stroke Cerebrovasc. Dis.* 2011;20:68-74
12. Carmichael ST. Rodent models of focal stroke: Size, mechanism, and purpose. *NeuroRx*. 2005;2:396-409
13. Brott T, Marler JR, Olinger CP, Adams HP, Jr., Tomsick T, Barsan WG, et al. Measurements of acute cerebral infarction: Lesion size by computed tomography. *Stroke*. 1989;20:871-875
14. Chen F, Suzuki Y, Nagai N, Jin L, Yu J, Wang H, et al. Rodent stroke induced by photochemical occlusion of proximal middle cerebral artery: Evolution monitored with mr imaging and histopathology. *Eur. J. Radiol.* 2007;63:68-75
15. Neumann-Haefelin T, Kastrup A, de Crespigny A, Yenari MA, Ringer T, Sun GH, et al. Serial mri after transient focal cerebral ischemia in rats: Dynamics of tissue injury, blood-brain barrier damage, and edema formation. *Stroke*. 2000;31:1965-1972; discussion 1972-1963
16. Chalela JA, Kasner SE. The fogging effect. *Neurology*. 2000;55:315
17. O'Brien P, Sellar RJ, Wardlaw JM. Fogging on t2-weighted mr after acute ischaemic stroke: How often might this occur and what are the implications? *Neuroradiology*. 2004;46:635-641
18. Zhang S, Murphy TH. Imaging the impact of cortical microcirculation on synaptic structure and sensory-evoked hemodynamic responses in vivo. *PLoS Biol.* 2007;5:e119

19. Murphy S, Rosli S, Acharya R, Mathias L, Lim R, Wallace E, et al. Amnion epithelial cell isolation and characterization for clinical use. *Curr. Protoc. Stem Cell Biol.* 2010;Chapter 1:Unit 1E 6
20. Fleming SM, Salcedo J, Fernagut PO, Rockenstein E, Masliah E, Levine MS, et al. Early and progressive sensorimotor anomalies in mice overexpressing wild-type human alpha-synuclein. *J. Neurosci.* 2004;24:9434-9440
21. Broughton BR, Lim R, Arumugam TV, Drummond GR, Wallace EM, Sobey CG. Post-stroke inflammation and the potential efficacy of novel stem cell therapies: Focus on amnion epithelial cells. *Front. Cell. Neurosci.* 2012;6:66
22. Bix GJ, Gowing EK, Clarkson AN. Perlecan domain v is neuroprotective and affords functional improvement in a photothrombotic stroke model in young and aged mice. *Transl Stroke Res*. 2013;4:515-523
23. Chan CT, Sobey CG, Lieu M, Ferens D, Kett MM, Diep H, et al. Obligatory role for b cells in the development of angiotensin ii-dependent hypertension. *Hypertension*. 2015;66:1023-1033
24. Courties G, Herisson F, Sager HB, Heidt T, Ye Y, Wei Y, et al. Ischemic stroke activates hematopoietic bone marrow stem cells. *Circ. Res.* 2015;116:407-417
25. Chu HX, Kim HA, Lee S, Moore JP, Chan CT, Vinh A, et al. Immune cell infiltration in malignant middle cerebral artery infarction: Comparison with transient cerebral ischemia. *J. Cereb. Blood Flow Metab.* 2014;34:450-459
26. Lee S, Brait VH, Arumugam TV, Evans MA, Kim HA, Widdop RE, et al. Neuroprotective effect of an angiotensin receptor type 2 agonist following cerebral ischemia in vitro and in vivo. *Exp. Transl. Stroke Med.* 2012;4:16
27. Baik SH, Fane M, Park JH, Cheng YL, Yang-Wei Fann D, Yun UJ, et al. Pin1 promotes neuronal death in stroke by stabilizing notch intracellular domain. *Ann. Neurol.* 2015;77:504-516

Stroke Online Supplement

Table I. Checklist of Methodological and Reporting Aspects for Articles Submitted to *Stroke* Involving Preclinical Experimentation

Methodological and Reporting Aspects	Description of Procedures
Experimental groups and study timeline	☑ The experimental group(s) have been clearly defined in the article, including number of animals in each experimental arm of the study. ☑ An account of the control group is provided, and number of animals in the control group has been reported. If no controls were used, the rationale has been stated. ☑ An overall study timeline is provided.
Inclusion and exclusion criteria	☑ A priori inclusion and exclusion criteria for tested animals were defined and have been reported in the article.
Randomization	☑ Animals were randomly assigned to the experimental groups. If the work being submitted does not contain multiple experimental groups, or if random assignment was not used, adequate explanations have been provided. ☑ Type and methods of randomization have been described. ☑ Methods used for allocation concealment have been reported.
Blinding	☑ Blinding procedures have been described with regard to masking of group/treatment assignment from the experimenter. The rationale for nonblinding of the experimenter has been provided, if such was not feasible. ☑ Blinding procedures have been described with regard to masking of group assignment during outcome assessment.
Sample size and power calculations	☑ Formal sample size and power calculations were conducted based on a priori determined outcome(s) and treatment effect, and the data have been reported. A formal size assessment was not conducted and a rationale has been provided.
Data reporting and statistical methods	☐ Number of animals in each group: randomized, tested, lost to follow-up, or died have been reported. If the experimentation involves repeated measurements, the number of animals assessed at each time point is provided, for all experimental groups. ☑ Baseline data on assessed outcome(s) for all experimental groups have been reported. ☑ Details on important adverse events and death of animals during the course of experimentation have been provided, for all experimental arms. ☑ Statistical methods used have been reported. ☑ Numeric data on outcomes have been provided in text, or in a tabular format with the main article or as supplementary tables, in addition to the figures.
Experimental details, ethics, and funding statements	☑ Details on experimentation including stroke model, formulation and dosage of therapeutic agent, site and route of administration, use of anesthesia and analgesia, temperature control during experimentation, and postprocedural monitoring have been described. ☑ Different sex animals have been used. If not, the reason/justification is provided. ☑ Statements on approval by ethics boards and ethical conduct of studies have been provided. ☑ Statements on funding and conflicts of interests have been provided.